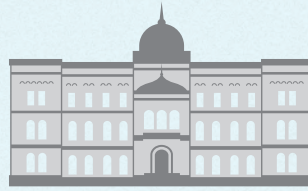


11th BALTIC
**MORPHOLOGY
MEETING**

NOVEMBER 13-15, 2024



ANATOMICUM, RIGA

11th Baltic Morphology Meeting

ABSTRACT BOOK

November 13–15, 2024
Rīga, Latvia



RĪGA STRADIŅŠ
UNIVERSITY

Baltic Morphology 11th Meeting [November 13–15, 2024]: Abstract Book. – Rīga: Rīga Stradiņš University, 2024. – 98 p., including Author Index.

<https://doi.org/10.25143/rsu-balt-morf-11-meeting>

Chair of the Meeting

Professor, *Dr. med.*, *Dr. habil. med.* Māra Pilmane

All abstracts reviewed

Abstracts do appear in the abstract book in accordance to their presentation order
(not in the alphabetical order)

Authors are responsible for the content of their abstracts

RSU IPD No. IPD-5115

© Rīga Stradiņš University, 2024
16 Dzirciema Street, Rīga, LV 1007

ISBN 978-9934-618-58-1 (printed edition)

ISBN 978-9934-618-59-8 (electronic edition, online)

Welcome greetings



Dear Distinguished Guests, Colleagues and Participants,

I am honoured to extend a gracious welcome to the Institute of Anatomy and Anthropology of the Rīga Stradiņš University for the 11th International Baltic Morphology Meeting. This event has become a cornerstone in the field of morphology. This meeting brings together leading experts and researchers from various countries and places to share their knowledge and insights.

Today, we stand on the brink of exciting discoveries that will shape the future of morphology. The 11th Baltic Morphology Meeting, with its unique ability to bridge disciplines and foster interdisciplinary collaboration, is not just a key player in this future, but a catalyst for it. By integrating knowledge from various fields, we can achieve a more comprehensive understanding of complex medical fields. I encourage all of you to take full advantage of this opportunity to share your knowledge, exchange ideas, and forge new collaborations. The discussions and interactions during this meeting can potentially lead to significant advancements in our understanding of morphology and its applications across different disciplines, thereby shaping the future of the field in ways we can only begin to imagine.

I wish all the attendees a productive and inspiring meeting. May your time here be filled with insightful discussions, new partnerships, and groundbreaking discoveries.

Thank you for your unwavering dedication, boundless passion, and invaluable contributions. Your efforts are shaping the future of morphology and inspiring others in the field. We are deeply grateful for your commitment and look forward to the groundbreaking discoveries that will emerge from this meeting.

AIGARS PĒTERSONS

Professor, *Dr. med.*, *Dr. habil. med.*,
Rīga Stradiņš University Rector



Dear colleagues and guests,

It is a great honour to welcome you to the 11th Baltic Morphology Meeting, a special gathering that has become a key tradition in our field since the restoration of independence. Riga proudly revived these meetings, and this year marks the fourth time it is hosted in our city, as well as the first time after the Covid-19 pandemic.

We are delighted to have participants from 11 countries, and over the next two intense days, we will enjoy 42 oral presentations and 40 posters. This year's meeting extends its focus beyond the Baltic region, showcasing important European collaborations and advancing morphology research across borders.

I am particularly thrilled to see so many young researchers contributing fresh perspectives and innovation to the field. Their involvement ensures a bright future for morphology.

Thank you for joining us in Riga, and I wish you a successful and inspiring conference.

Warm regards,

JANA PAVĀRE
Professor, *Dr. med.*,
Dean of Faculty of Medicine,
Rīga Stradiņš University



Distinguished Guests, Colleagues, and Friends,

Good afternoon and welcome to the 11th Baltic Morphology Meeting here in the beautiful city of Riga and in the old and modern at the same time Anatomicum! It is my great pleasure to extend a warm welcome to each and every one of you.

First and foremost, I would like to express our deepest gratitude to all who have traveled from near and far to join us for this gathering, that's renewed again after the Covid pandemia. Your commitment to advancing the field of morphology is truly inspiring. This year's meeting promises to be an exciting and enriching experience.

Our gathering is not only about sharing knowledge but also about building connections and strengthening the bonds within our professional community. May this meeting be a source of inspiration, growth, and long (life) lasting connections! May you have time to look also at Riga and our historical expositions of Anatomicum/Museum of Anatomy and enjoy the points where the previous 100 years' values meet the nowadays usage!

Once again, welcome to Riga and the 11th Baltic Morphology Meeting. I wish you a successful and memorable conference.

MĀRA PILMANE

Professor, *Dr. med., Dr. habil. med.*

Director, Institute of the Anatomy and Anthropology

Head, Department of Morphology

Rīga Stradiņš University

Full member, Latvian Academy of Sciences

Organizing committee



Head of the Meeting – Professor **Māra Pilmane**
Director of the Institute of Anatomy and Anthropology,
Rīga Stradiņš University, Full member of the Latvian
Academy of Sciences.



Meeting secretary – **Līga Hartpēnga**
Experienced project manager with a demonstrated history of
working in the event industry, Rīga Stradiņš University.



Member of the Meeting organising committee –
Associate professor **Dzintra Kažoka**
Human anatomy tutor and coordinator of the Study (Anatomy)
Division at the Department of Morphology of the Institute of
Anatomy and Anthropology, Rīga Stradiņš University.



Member of the Meeting organising committee –
Assistant professor **Anna Junga**
Researcher at the Institute of Anatomy and Anthropology,
assistant professor of the Department of Morphology and head
of the Laboratory of Morphology, Rīga Stradiņš University.



Meeting coordinator – **Daiga Enkuzena**
Daiga Enkuzena has been holding the office manager's
position at the Institute of Anatomy and Anthropology,
Rīga Stradiņš University.



Meeting coordinator – **Dārta Cīrule**
Dārta Cīrule joined the Department of Morphology,
Rīga Stradiņš University, as a study process coordinator.

Scientific committee



Professor **Māra Pilmane**, *Dr. med, Dr. habil. med.*
Head of the Meeting, Director of the RSU Institute
of Anatomy and Anthropology.
Full member of the Latvian Academy of Sciences.



Professor **Jānis Vētra**, *Dr. habil. med.*
RSU Institute of Anatomy and Anthropology.



Associate professor **Dzintra Kažoka**, *Dr. med.*
Human anatomy tutor and coordinator of the Study (Anatomy)
Division at the Department of Morphology of the RSU Institute
of Anatomy and Anthropology.



Andrejs Ivanovs, MD, MSc, PhD, MRCP(UK), FRCPath
Consultant haematologist at the Edinburgh Cancer Centre, a tertiary
care oncology centre in Scotland. Dr. Ivanovs is specialising in
lymphoid malignancies and cellular immunotherapy.

Contents

WELCOME GREETINGS	3
INVITED LECTURERS	13
Ionizing radiation and the eye: epidemiological studies and new approaches to correlating functional and morphological damage <i>Fedirko P., Pilmane M.</i>	14
Immunophenotype and gene expression analysis of the earliest human haematopoietic stem cells <i>Ivanovs A.</i>	15
Neuroanatomy of the heart <i>Pauža D. H.</i>	16
Vascular variations at abdomen and thorax: description of three main topics as the important aspects of clinical anatomy <i>Polgij M.</i>	17
“Deus ex Machina” or moving sculptures in the interior of Lutheran churches of Latvia <i>Spārītis O.</i>	18
Exploring the black box of human reproduction – the role of uterine (endometrial) Natural Killer cells in embryo implantation: from histology, through recurrent implantation failure and to future clinical perspectives <i>Varga I., Lapides L., Babal P.</i>	19
Anatomical body donation in Europe: history and ethical challenges <i>Winkelmann A.</i>	20
Alzheimer’s disease and vitamin D related pathways <i>Yilmazer S., Gezen Ak D., Dursun E.</i>	21
ORAL PRESENTATIONS	23
Cholinergic and adrenergic nerve fibers in frog heart <i>Batulevičius D., Skripkienė G., Levin D., Skripka V.</i>	24
Morphological comparison of paediatric and adult acquired cholesteatoma <i>Dambergs K., Segliņa G., Pilmane M.</i>	25
3D Gaussian Splatting for real-time radiance field rendering in anatomy education and 3D model creation <i>Edelmers E.</i>	26
The impact of neuronal ion channels in epilepsy: a current overview <i>Groma V., Naumovs V., Skuja S.</i>	27
Comparative study of sodium-dependent glucose co-transporters in kidneys in norm and in T-2 mycotoxicosis <i>Hussar P., Allmang C., Popvska-Percinica F., Dūrītis I., Jārveots T.</i>	28
Insights for the usage of rats, rabbits and pigs as animal models in the improvement of treatment methods for heart arrhythmia <i>Inokaitis H., Paužienė N., Pauža D. H.</i>	29

Shortening of the gestational age of newborns during 1995–2020 period: analysis of Lithuanian medical data of births <i>Jakimaviciene E. M., Isakova J., Stasiunas A., Tutkuvienė J.</i>	30
Evaluation of TGFβ1, HGF, FGF-2, FGFR1 and apoptosis in placentas of various gestational ages <i>Junga A., Pilmane M.</i>	31
Variations of the sensory nerves of the dorsal aspect of the forearm and hand <i>Kachlik D., Khadanovich A., Herma T., Benes M., Kaiser R.</i>	32
Enhancing anatomy course with “Anatomage” radiological images: modules and implementation strategies <i>Kažoka D., Pilmane M.</i>	33
The association of neutrophil-to-lymphocyte ratio with in-hospital mortality in COVID-19 patients <i>Merkurjeva K., Vidusa L., Štrumfs B., Uljanovs R., Štrumfa I.</i>	34
Cardiovascular paleopathology in Lithuanian historical populations: evidence from mummified and skeletal remains <i>Mialkowskyj D., Jankauskas R., Kozakaitė J., Piombino-Mascalì D.</i>	35
Comparison of body mass index, body image and self-esteem among women aged 25–65 before COVID-19, during the first and second quarantine in Lithuania <i>Misiute A., Tutkuvienė J., Nedzinskiene L.</i>	36
Characterization of tissue immunity defense factors of the lip in primary dentition children with Bilateral Cleft Lip Palate <i>Ozola L., Pilmane M.</i>	37
Facial cleft basic research in Latvia: search for the best methods and directions <i>Pilmane M.</i>	38
Understanding the impact of chronic hypertension on cardiac autonomic innervation from the end of life perspective <i>Ranceviene D., Rysevaite-Kyguoliene K., Sabeckis I., Paužienė N.</i>	39
Nerve supply of aorta in rats <i>Rekke K., Rysevaite-Kyguoliene K., Onashko Y., Sabeckis I., Pauža D. H., Khmel O.</i>	40
Comparative anatomy of the epicardial ganglionated nerve plexus in two pig breeds <i>Saburkine I., Rysevaite-Kyguoliene K., Ranceviene D., Rekke K., Paužienė N., Khmel O., Pauža D. H.</i>	41
Cartilage degradation and synovial inflammation in osteoarthritis progression: morphological and molecular analysis <i>Semenistaja S., Sokolovska L., Studers P., Kadiša A., Groma V., Skuja S.</i>	42
Dynamics of general size and shape of the craniofacial compartment, and its sexual differences in Lithuanian adolescents, taking into account the pubertal growth spurt <i>Stukaite-Ruibiene E., Tutkus J., Gervickaite S., Šimkūnaitė-Rizgelienė R., Barkus A., Tutkuvienė J.</i>	43
Etiopathogenetic mechanisms of vocal nodules and Reinke’s edema development and their morphopathological manifestations <i>Sumerags D., Pilmane M., Segliņa G.</i>	44
Radiomorphometric assessment of posterior condylar canals in children at the age between 2 months and 14 years <i>Szeliga S., Drożdż A.</i>	45

Role of maternal undernutrition: comparison of histomorphological changes in visceral organs and retinas of two-generation rat offspring <i>Šimkūnaitė-Rizgeliė R., Laurinavičiūtė G., Reivytytė R., Virbauskytė V., Semenkovaite J., Šlažaitė G., Strelchenko J., Vosyliūtė R., Žalgevičienė V., Čepulienė R., Bartuškienė V., Tutkuvienė J.</i>	46
Tumour microenvironment in solid and haematological malignancies <i>Štrumfa I., Šinkarevs S., Štrumfs B., Sperga M.</i>	47
Modern light microscopy techniques: overcoming the diffraction limit <i>Štrumfs B., Šinkarevs S., Uljanovs R., Štrumfa I.</i>	48
Dynamics in the eyes, nose and lips areas of Lithuanian men from 4 to 30 years of age in relation to the size and shape of the craniofacial complex <i>Tutkus J., Gervickaite S., Barkus A., Tutkuvienė J., Šimkūnaitė-Rizgeliė R.</i>	49
Secular trend in general size and shape parameters of head and face of Lithuanian adolescents during 1965–2015 period <i>Tutkuvienė J., Gervickaite S., Tutkus J., Stukaite-Ruibiene E., Barkus A., Almonaitiene R., Šimkūnaitė-Rizgeliė R.</i>	50
Hotspot pattern in parathyroid pathology: implications for pathogenesis and diagnostics <i>Uljanovs R., Vidusa L., Štrumfs B., Merkurjeva K., Štrumfa I.</i>	51
Investigation of genes and gene proteins in cleft affected tissue <i>Vaivads M., Akota I., Pilmane M.</i>	52
Research ethics of morphological studies <i>Vētra J.</i>	53
Endotypes of chronic rhinosinusitis with primary and recurring nasal polyps in the Latvian population <i>Vīksne R. J., Segliņa G., Pilmane M.</i>	54
Evaluation of immunomodulatory tissue factors in gallbladders of pediatric patients with calculous cholecystitis <i>Zariņa K. Z., Pētersons A., Pilmane M.</i>	55
A case study on the pulmonary arterial tree: detailed anatomical and topographical analysis <i>Zicāns M., Kažoka D., Skride A., Pilmane M.</i>	56
POSTER PRESENTATIONS	57
Differences in expression of Defensin-3, Defensin-2, LL-37, Galectin-10, CD163 in oral mucosa of control group and patients with chronic periodontitis <i>Apele Z., Pilmane M.</i>	58
Analysis of arm span to height ratio in Latvian residents from different regions based on 1930s data <i>Asare L., Vētra J., Ivanovs A.</i>	59
Mastering epoxy resin for educational model creation <i>Bode M., Strance Ğ., Kažoka D.</i>	60
Characterization of the pro-inflammatory, regulatory and anti-inflammatory cytokines of placenta in different gestation times <i>Brikune E., Pilmane M.</i>	61
Differences of tissue factors in bone and cartilage between first-time and re-operated patients affected by facial clefts <i>Buile D., Pilmane M., Akota I.</i>	62

In-person and remote anatomy studies, application of digital tools in anatomy teaching: a comparative study <i>Čepulienė R., Miliauskienė Z., Tutkus V., Šimkūnaitė-Rizgelienė R., Vosyliute R., Nedzinskiene L., Tutkuvienė J.</i>	63
Experimental comparative study of dichloroacetate salts and temozolomide effects on pediatric glioblastoma in vivo and in vitro <i>Damanskienė E., Balnytė I., Valančiūtė A., Stakišaitis D.</i>	64
Growth factors in the wall of anomalies-affected gallbladder of children <i>Derbeņeva D., Pilmane M., Pētersons A.</i>	65
Lung cancer cell tumors respond differently to the treatment with sodium valproate in the chicken embryo chorioallantoic membrane model <i>Diržiuviene R., Šlekiene L., Palubinskienė J., Balnytė I., Lasiene K., Stakišaitis D., Valančiūtė A.</i>	66
Deep learning-based software for automated cell detection and counting in whole-slide histological image analysis <i>Edelmers E., Fišere I.</i>	67
Changes in the vitreous body in residents of radiation-contaminated areas in the early period after a radiation disaster <i>Fedirko P., Pilmane M., Babenko T., Garkava N., Dorichevska R.</i>	68
Craniofacial metrics of children aged 1–15 years in Latvia <i>Grabčika A., Kažoka D., Vētra J.</i>	69
CAM-Delam – an in vivo assay to visualize and quantify the delamination and invasion capacity of human cancer cells <i>Green T., Šlekiene L., Gunhaga L.</i>	70
Histological analysis of chondrosarcoma in an uncommon cranial location: a case report <i>Jakovļevs A.</i>	71
Effects of long-term treatment with a combination of valproic acid and sodium dichloroacetate in rats <i>Juknevičienė M., Balnytė I., Valančiūtė A., Stakišaitis D.</i>	72
Human olecranon parameters and shapes variability: insights from “Anatomage” study <i>Kažoka D., Pilmane M.</i>	73
Variability in ear morphology among virtual human bodies: insights from digital measurements <i>Kažoka D., Pilmane M.</i>	74
Exploring the diverse branching patterns of Arbor Vitae <i>Kuļibaba G., Kažoka D.</i>	75
Morphological changes of angiotensin II type 2 receptor at myenteric plexuses of diverticular disease in the human gastrointestinal tract <i>Lapeikis I., Rysevaitė-Kyguoliene K., Malinauskas M., Paužienė N.</i>	76
Morphometrical parameters of 31–35-year-old men testes <i>Lasiene K., Radzeviciute S., Gasiliunas D., Juodziukyniene N., Žilaitiene B., Dabužinskiene A.</i>	77
Results of arterial blood pressure in pre-school aged children in Riga region <i>Martinsone-Bērzkalne L., Umbraško S., Asare L.</i>	78
Spatially and temporally restricted expression of BMP-2 and Shh during early development of human embryo spinal cord <i>Namm A., Arend A., Torga T., Aunapuu M.</i>	79
Expression of NaV1.2 in the hippocampus and cerebellum of epilepsy patients <i>Naumovs V., Skuja S., Groma V.</i>	80

A pilot study of cells in human plantar fascia exposed to chronic ischemia due to atherosclerosis <i>Palubinskienė J., Gorodetsky M. L., Kilimaitė E., Lekšas M.</i>	81
Morphopathogenic factors of neonate intra-abdominal adhesions: a pilot study <i>Pauliņš A., Pilmane M.</i>	82
Comparison of healthy and diseased free-stall barn cow milk microbiota, cytokines and antimicrobial proteins in seasonal aspect <i>Pilmane M., Lohova E., Meldēris I., Gontar L., Kochanski M., Drutowska A., Prieto-Simon B.</i>	83
Body donation in Latvia during the last 30 years <i>Pilmane M., Kažoka D., Vētra J., Gardovskis J., Pētersons A.</i>	84
Distribution of genes and their proteins in Ladd's band tissue <i>Pivriķa E., Pētersons A., Junga A., Pilmane M.</i>	85
Effect of multi-stressor training on the antioxidative system <i>Pļaviņa L.</i>	86
Changes in neuropeptides expression in the jugular and nodose ganglion of the vagus nerve in arterial hypertension during the age <i>Rysevaite-Kyguoliene K., Novikova J., Paužienė N.</i>	87
Galectin-10 characterization in cleft lip palate (CLP) – affected palatal tissue <i>Rone A. E., Pilmane M.</i>	88
Abundance, morphology and innervation of cardiac small intensely fluorescent cells <i>Sabeckis I., Rysevaite-Kyguoliene K., Pauža D. H.</i>	89
Effects of environmentally relevant concentrations of phthalates on first generation rat embryo body and bone length <i>Sėrikovaitė E., Alčauskaitė J., Paulikaitė E., Skujienė G., Žalgevičienė V., Aukštikalnienė R.</i>	90
A comparative study of effectiveness of sodium dichloroacetate and temozolomide on glioblastoma xenograft growth <i>Skredenīene R., Stakišaitis D., Valančiūtė A., Balnytė I.</i>	91
The expression of collagen neoepitope C2C in the articular cartilage and its relation with joint tissue damage in patients with knee osteoarthritis <i>Torga T., Suutre S., Kisand K., Aunapuu M., Arend A.</i>	92
Radiological insights into chronic Pelvic Congestion Syndrome and May-Thurner Syndrome: a comparative study of selected cases in Latvia <i>Trošins D., Kratovska A., Kažoka D., Pilmane M.</i>	93
Analysis of indices of children's physical development in a longitudinal study <i>Umbraško S., Martinsone-Bėrzkalne L., Edelmērs E., Asare L.</i>	94
Distribution of immunomodulation, protection and regeneration factors in cleft affected bone and cartilage <i>Vaivads M., Pilmane M.</i>	95
Chronic stress impact on pancreas morphology in type 1 diabetes mellitus <i>Vosyliūtė R., Achahbar Charki H., Šimkūnaitė-Rizgelienė R., Bikulčienė I., Baleišis J., Rudys R., Tutkuvienė J.</i>	96
AUTHORS	97



Invited lecturers

Ionizing radiation and the eye: epidemiological studies and new approaches to correlating functional and morphological damage

Fedirko Pavlo¹, Pilmane Māra²

¹*Laboratory of Radiation Induced Eye Diseases, Institute of Radiation Hygiene and Epidemiology of National Research Center for Radiation Medicine of National Academy of Medical Sciences of Ukraine*

²*Institute of Anatomy and Anthropology, Rīga Stradiņš University, Latvia*

Objectives. Medical assistance to victims of ionizing radiation influence, first of all in relatively low doses, should be based on a clear understanding of the mutual relationship of organic and functional changes that are formed as a result of radiation exposure. We studied the peculiarities of the appearance of morphological and functional changes in the eye caused by radiation exposure, using the data of previously conducted examinations.

Materials and methods. The results of long-term follow-up cohorts of participants of emergency work in the Chornobyl zone (1170 people) in 1993–1998 and results of ophthalmologic examinations of 112 participants of emergency work in the Chornobyl zone conducted in 1992 were re-analyzed.

Results. The initial signs of macular degeneration in radiation-exposed individuals were manifested by minimal changes in the morphology of the retina and choroid (6 years after radiation exposure – in 20.5% of the examined) and absence a decrease in central vision. A decrease in visual functions was observed later. Clouding of the lens, mainly on the periphery, is initially detected only during examination (6 years after radiation exposure – in 29.5% of the examined) and does not cause changes in visual functions. Changes in the retinal vessels were also initially detected only during an ophthalmological examination.

Conclusions. The results of the reanalysis of previously conducted ophthalmological studies of radiation-exposed persons showed that in the presence of pronounced morphological changes in the structures of the eye, but visual functions are preserved for a long time. There is every reason to believe that the development of such pathological processes as cataracts, age-related macular degeneration, small vessel disease occurs as a result of the appearance of morphological changes already in the early period after radiation exposure, and functional changes are a relatively remote consequence of organic disorders.

Immunophenotype and gene expression analysis of the earliest human haematopoietic stem cells

Ivanovs Andrejs

Edinburgh Cancer Centre, United Kingdom

Objectives. First human transplantable haematopoietic stem cells (HSCs) emerge in the aorta-gonad-mesonephros (AGM) region of the embryo during Carnegie stages 14–17. To date, the best enrichment of the earliest AGM region-derived HSCs yields 1 HSC per 500–3,000 CD34⁺ VE-CAD⁺ CD45⁺ cells. This large population contains mostly more mature progenitors rather than true HSCs and not suitable for a gene expression analysis. We investigated here whether additional surface antigens expressed in developing HSCs can be employed for a more efficient purification of the human earliest HSCs.

Materials and methods. Human embryos were obtained immediately after medical elective termination of pregnancy. Informed written consent to use the samples in research was obtained from patients. Cell populations of interest were purified and characterised immunophenotypically and functionally using a long-term repopulation assay by transplantation into irradiated adult NOD.Cg-Prkdc^{scid} Il2rg^{tm1 Wjl/Sz} (NSG) mice. Datasets for a bioinformatics analysis were downloaded from the NCBI Gene Expression Omnibus.

Results. We characterised the VE-CAD⁺ CD45⁺ population in the human AGM region enriched for HSCs, using CD41 and CD43, known to be expressed in developing mouse HSCs, and GPI-80, a marker of mid-trimester human foetal liver HSCs. We found that VE-CAD⁺ CD45⁺ population contains two HSPC clusters one of which is less proliferative and has a more prominent HSC molecular signature. Although single cell co-expression analysis has not revealed association of CD41 or CD43 with the HSC signature, functional long-term transplantation experiments showed that definitive HSCs are CD43⁺ CD41⁻ GPI-80.

Conclusions. We showed that the first definitive HSCs emerging in the human AGM region, in addition to previously determined markers also express CD43⁺ but not CD41 (labels developing mouse HSCs) or GPI-80 (labels mid-trimester human HSCs). A deeper analysis of transcription signature of these cells along with functional studies will aid better understanding of underlying mechanisms driving HSC development and potentially facilitate HSC generation from pluripotent stem cells for clinical needs.

Neuroanatomy of the heart

Pauža Dainius Haroldas

*Institute of Anatomy, Faculty of Medicine,
Lithuanian University of Health Sciences, Lithuania*

Objectives. The presentation aims to disclose the neuroanatomy of the mammalian hearts.

Materials and methods. To demonstrate differences in cardiac neuroanatomy, the hearts of laboratory mammals, dogs, pigs, sheep, and humans were stained for neural tissues (acetylcholinesterase histochemistry, immunohistochemistry for diverse neuropeptides) and analyzed by diverse techniques of microscopy (stereo, fluorescent, confocal, and electron microscopy) during the last 30 years.

Results. Sympathetic, parasympathetic and sensory axons within mediastinal nerves access the heart through the cardiac hilum. In the epicardium, the nerves form the dense ganglionated neural plexus that may be considered as being split into 5–7 portions (subplexuses) by atrial auricles, sinuses of the great veins and roots of the aorta and pulmonary trunk. Five epicardial ganglionated subplexuses proceed from the venous part of the heart hilum, while nerves, passing the arterial part of the heart hilum, extend on the walls of cardiac ventricles via two coronary subplexuses. The richest in epicardial ganglia areas are concentrated on the root of the superior vena cava and the inferior surface of the left atrium. Depending on animal species and age, the epicardial ganglia may averagely involve up to 100 thousand intrinsic neuronal somata, from which postganglionic axons extend to the target cells in all heart wall layers. It's generally ratified that both the cardiac anatomy and the pattern of coronary blood supply are similar in most mammalian species, including the human one. However, there is no attitude regarding the neuroanatomy of the heart. Comparative anatomy demonstrates principal differences between cardiac neuroanatomy of the examined animals and humans although the general schema of the intrinsic cardiac nervous system is comparable in animals and humans.

Conclusions. The discovered differences in the morphologic pattern of intrinsic nerve plexus within the examined human and animal hearts suggest that the human hearts are neuroanatomically unique and differ from the hearts of many animals.

Vascular variations at abdomen and thorax: description of three main topics as the important aspects of clinical anatomy

Polgaj Michał

*Department of Normal and Clinical Anatomy, Chair of Anatomy and Histology,
Medical University of Lodz, Poland*

Objectives. The aim of the invited lecture is the presentation of the most important vascular variations at abdomen and thorax.

Materials and methods. A review of several databases like PubMed and EBSCO was performed. A comprehensive analysis of knowledge describing the aberrant right subclavian artery, the nutcracker syndrome and supernumerary (multiple) renal arteries has been made.

Results. The aberrant right subclavian artery (usually name as the arteria lusoria) is the first variation. In such variation the brachiocephalic trunk is absent, and four huge arteries arise from the aortic arch are (from right to left side): the right common carotid artery, the left common carotid artery, the left subclavian artery, and the final on distal left sided origin, the right subclavian artery (name as aberrant right subclavian artery – arteria lusoria). If this artery compresses the adjacent anatomical structures, different symptoms like dysphagia, dyspnea, cough, and retrosternal pain can be presented. The nutcracker syndrome is the second one. There are a few types of the syndrome, and the most common situation is when the left renal vein during its pathway is compressed between the superior mesenteric artery and the abdominal aorta. The clinical symptoms are generally divided into renal presentation or urologic presentation. Supernumerary (multiple) renal arteries are the third variation. Usually, kidney is supplied by only one renal artery. However, often there are more than one artery for vascularization of kidney. Such information is of particular importance, especially for surgeons, nephrologists, intervention radiologists, and vascular surgeons.

Conclusions. Knowledge of the presented vascular variations has grown in importance with the increasing number of surgical and vascular interventions, various vascular reconstructions and radiological techniques performed in recent years. The lecture offers comprehensive description of the most important clinical and morphological aspects related to mentioned above vascular variations.

“Deus ex Machina” or moving sculptures in the interior of Lutheran churches of Latvia

Spārītis Ojārs

Academy of Arts of Latvia, Latvia

Objectives. The term “Deus ex Machina” was used in ancient Greek and Roman theater performances as stage machinery and referred to the temporary appearance of a hero or god to unravel and resolve a hopeless situation. The current paper characterizes the appearance, function and use of moving sculptures – automata – in Latvian baroque church interiors.

Renaissance science sparked developments in mathematics, astronomy, and mechanics that stimulated not only the invention of curiosities, but also the construction of practical mechanisms and tools. Knowledge transfer from mechanics to applied and fine arts brought moments of mystery and wonder in the fields of performing arts, and the spheres of representativity and liturgy. The use of automatons helped to invent new mechanisms, making the mechanical movement of “animated sculptures” an attractive public entertainment.

Both written evidence and artifacts preserved in museums and churches bear witness to the social demand for the integration of theatrical elements into the formerly conservative environment – of, for example, the church. Drawing inspiration from the culturally linked region of former Prussia, the current paper concentrates on moving figures in interior space of Lutheran churches in Latvia to expose the variety of fascinating objects, including organ facades and baptismal fonts.

Keywords: Deus ex Machina, automaton, church, theater, mechanic, moving sculpture, baptismal font.

Materials and methods. On original evidences based historical survey.

Results. Identification of succession in content, morphology and form.

Conclusions. In the field of history of culture, tangentially touching history of medicine.

Exploring the black box of human reproduction – the role of uterine (endometrial) Natural Killer cells in embryo implantation: from histology, through recurrent implantation failure and to future clinical perspectives

Varga Ivan, Lapidés Lenka, Babal Pavel

Faculty of Medicine, Comenius University in Bratislava, Slovakia

Objectives. In recent years, views on the importance and functioning of the immune system during blastocyst implantation, and subsequent pregnancy have changed significantly. Uterine Natural Killer (uNK) cells correspond to large granular lymphocytes and belong to innate immunity. The uNK cells are sporadically present in the endometrium during the proliferative and early secretory phases. But uNK cells are the most abundant cell type at the maternal–fetal interface during early pregnancy, and they represent 70% of uterine leukocytes. The exact mechanisms of how uNK cells may contribute to normal implantation but also to recurrent miscarriages are still obscure and elusive.

Materials and methods. Study of archival sources as well as a comprehensive review of recent textbooks of histology and summary of our previously published results on histological analysis of endometrial samples from women with habitual abortion and recurrent implantation failure. Samples were collected between days 19 and 21 of the menstrual cycle, mainly by Pipelle endometrial sampling. The samples were further processed for immunohistochemistry using anti-CD56 to visualize this antigen marker of uNK cells.

Results. Based on our results, there is a correlation between habitual abortion and recurrent implantation failure, idiopathic sterility, endometriosis, and uNK cell count.

Conclusions. uNK cell research needs to address several issues before it can be implemented clinically, namely the standardization of uNK cell evaluation, more profound insights into how uNK cells contribute to immune homeostasis and immune suppression, and how exactly they interact with all the components of the decidua during pregnancy, and finally yet importantly, the development of a precise methodology of uNK cell targeting within the state-of-the-art immune therapy of pregnancy-related conditions.

Acknowledgement. This research was funded by a grant from The Slovak Ministry of Education (No. VEGA 1/0625/23), entitled “Immunologically active endometrial cells in the context of embryo implantation and their targeting in the treatment of infertility”.

Anatomical body donation in Europe: history and ethical challenges

Winkelmann Andreas

Medical School Brandenburg, Germany

Objectives. Body donation is based on an informed consent of individuals during their lifetime bequeathing their bodies to anatomical use after death. The history of body donation has not been researched in much detail for most countries in Europe. Body donation, in today's sense, was mostly introduced from the 1960s onwards. Germany's history in this respect may serve as an example as it includes an Eastern and Western context.

Materials and methods. Historical research and analysis of the current situation.

Results. In the times of the "Third Reich", German anatomists largely benefitted from the high execution numbers of an infamous justice system. This gave way to a shortage of bodies after 1945. It proved difficult to return to pre-war procedures of body acquisition, mainly using bodies of those who could not afford burial and unclaimed bodies. Nevertheless, it took another 15 to 30 years until anatomists turned towards body donation as a relevant source. In West Germany, from the late 1970s most anatomists relied exclusively on body donation. In East Germany, this took until after 1989. Only in the 1990s laws to this effect were installed, if only in some federal states. In Europe, the situation is far from homogeneous. Most West European anatomists now rely solely on donated bodies, while some East European anatomists still accept unclaimed bodies.

Conclusions. The still patchy situation in Europe regarding body donation may be partly explained by different historical developments, particularly between East and West Europe. Even with established and well-functioning body donation programs, ethical challenges persist, like the question of how detailed the informed consent of the donors should cover later use of their bodies, or of how to deal with anatomical collections from times without informed consent.

Alzheimer's disease and vitamin D related pathways

Yilmazer Selma¹, Gezen Ak Duygu², Dursun Erdinc²

¹ Faculty of Medicine, Halic University, Turkey

² Brain and Neurodegenerative Disorders Research Laboratories Department of Neuroscience
Institute of Neurological Sciences, Istanbul University, Turkey

Objectives. Our group has focused on the vitamin D pathways that are involved in neurodegeneration, given the specific functions of this hormone on calcium metabolism and its role in gene regulation. The human studies in our group uncovered the association between VDR and AD for the first time. These findings were also confirmed with genome wide association (GWA) data. Fewer studies have been conducted on the molecular basis of the vitamin D-neurodegeneration relationship.

Materials and methods. In our in vitro studies amyloid beta which participates in the pathogenesis of AD, was applied to cortical neurons in culture to create an in vitro Alzheimer's Disease model. Effects of vitamin D receptor (VDR) gene silencing were also investigated in primary neuronal cultures.

Results. Our experiments indicated that beta amyloid triggers a neurodegeneration mechanism not only by inducing the expression of L-type voltage sensitive calcium channels (LVSCC) and altering nerve growth factor (NGF) synthesis but also by significantly suppressing the expression of VDR and inducing 25-hydroxyvitamin D3 24 hydroxylase (24OHase), the enzyme that accelerates vitamin D catabolism. in cultured cortical neurons. This finding supplied us a novel perspective for explaining the basis of neurodegeneration mechanisms in AD.

The same alterations observed in independent experiments as response to VDR silencing and the alterations normalized with vitamin D treatment and proved that the disruption of vitamin D-VDR pathway could act on the same mechanisms which cause neurodegeneration.

These studies were the first to indicate the direct effect of one of the pathological hallmarks of AD on VDR and vitamin D metabolism. We have also reported that LVSCC-A1C, NGF and inducible nitric oxide synthase (iNOS) are regulated by VDR.

Conclusions. We have suggested that AD might be a consequence of a hormonal imbalance in which the critical hormone is 1,25-dihydroxyvitamin D3.



Oral presentations

Cholinergic and adrenergic nerve fibers in frog heart

Batulevičius Darius, Skripkienė Gertrūda, Levin Denis, Skripka Valdas

*Faculty of Medicine, Institute of Anatomy,
Lithuanian University of Health Sciences, Lithuania*

Objectives. 1. To map the cholinergic and adrenergic nerve fibers in frog atrial whole mounts. 2. To evaluate the fluorescence intensities and 2D areas of cholinergic and adrenergic nerve fibers in extended focus images of frog intracardiac nerves. 3. To check if our measured values differ in several regions of frog heart.

Materials and methods. Common frogs, *Rana temporaria*, have been used for this study. Atrial whole mounts were prepared and stained immunohistochemically for choline acetyltransferase (ChAT) and tyrosine hydroxylase (TH). Extended focus images were obtained by confocal laser scanning and fluorescent microscopy. In fragments of extended focus images, we measured the following values: (1) fluorescence intensities of ChAT and TH positive fibers expressed as integrated densities in Image J software and (2) percentages of 2D areas occupied by ChAT and TH positive fibers.

Results. Average integrated densities of ChAT and TH positive fibers did not differ significantly (Mean \pm SE $\times 10^6$, 45.4 ± 7.6 vs. 33.9 ± 5.7 ; $P = 0.268$). Percentage of area occupied by ChAT positive and TH positive fibers also did not differ significantly (74.4 ± 2.7 vs. 80.7 ± 1.6 ; $P = 0.123$). Average ratio of integrated densities between ChAT positive and TH positive fibers was 1.38 ± 0.10 . Average ratio of percentages of 2D areas occupied by ChAT positive and TH positive fibers was 0.93 ± 0.03 . We did not find significant differences of investigated values within several cardiac regions examined.

Conclusions. Our findings imply that both cholinergic and adrenergic fibers are distributed in major intracardiac nerves of frog. Proportional distribution of cholinergic and adrenergic fibers in frog intracardiac nerves is similar with respect to (1) amounts of neurochemicals ChAT and TH, and (2) areas the ChAT and TH positive fibers occupy. Our data contrasts to reports on mouse and rat heart where predominantly cholinergic or adrenergic nerves were reported.

Morphological comparison of paediatric and adult acquired cholesteatoma

Damberg Kristaps¹, Segliņa Gunta¹, Pilmane Māra²

¹Department of Otorhinolaryngology, Rīga Stradiņš University, Latvia

²Department of Morphology, Institute of Anatomy and Anthropology, Rīga Stradiņš University, Latvia

Objectives. Complex characterisation of remodelling, proliferation, inflammation, local defence, angiogenesis, and relative amount and distribution of the SHH gene protein of the cholesteatoma tissue in an ontogenetic aspect.

Materials and methods. Tissues were obtained from 25 children and 25 adults during cholesteatoma surgery. Tissues were immunohistochemically stained for MMP-2, MMP-9, TIMP-2, TIMP-4, Ki-67, NF- κ B, IL-1, IL-10, H β D-2, H β D-4, VEGF, SHH. The slides were analysed by light microscopy using a semi-quantitative method. Kruskal-Wallis's test was used to detect statistical differences between groups.

Results. On average, a few to moderate (+/++) MMP-2; an occasional (0/+) MMP-9; a few(+) TIMP-2; moderate to numerous (+/+++) TIMP-4; an occasional (0/+) Ki-67; a moderate (++) number of NF- κ B; a few to moderate (+/++) IL-1, IL-10 and H β D-2; an occasional (0/+) H β D-4; few to moderate (+/++) VEGF and moderate to numerous (+/+++) SHH positive cells were observed in adult and paediatric cholesteatoma.

There were no statistically significant differences in all cell factors between both groups.

Similar correlations were observed in both study groups between MMP-2 in matrix and perimatrix ($r = 0.574$ adults, $r = 0.803$ children), MMP-2 matrix and TIMP-2 matrix ($r = 0.484$ adults, $r = 0.622$ children); MMP-9 perimatrix and TIMP-4 perimatrix ($r = 0.664$ adults, $r = 0.490$ children); MMP-2 matrix and SHH matrix ($r = 0.719$ adults, $r = 0.786$ children); IL-1 matrix and IL-10 matrix ($r = 0.813$ adults, $r = 0.709$ children); IL-10 matrix and H β D-2 matrix ($r = 0.841$ adults, $r = 0.828$ children).

Conclusions. Variable expression of remodulation factors (increased MMP-2 and TIMP-4, while decreased MMP-9 and TIMP-2) in cholesteatoma tissues indicates imbalance of non-age related remodulation factors.

The tendency to increase the number of positive structures of IL-1 α and the tendency to decrease the number of positive cells of IL-10 in cholesteatoma tissue indicate a tumour-specific, overall pro- and anti-inflammatory cytokine imbalance.

The increased amount of SHH positive cells in the cholesteatoma perimatrix indicates the intensification of this gene protein in tumour growth.

3D Gaussian Splatting for real-time radiance field rendering in anatomy education and 3D model creation

Edelmers Edgars

Institute of Anatomy and Anthropology, Rīga Stradiņš University, Latvia

Objectives. This thesis examines the use of 3D Gaussian Splatting for real-time radiance field rendering in anatomy education and 3D anatomical model creation. The technique aims to enhance anatomical education through real-time, high-quality visualization of medical imaging data, providing interactive 3D models for improved learning and exploration.

Materials and methods. The method leverages medical imaging data, such as MRI and CT scans, to create 3D radiance fields. These are rendered using a novel 3D Gaussian representation that optimizes the scene through anisotropic Gaussians. The process involves three stages:

- 1) Data preprocessing: Initial sparse point clouds are generated from medical imaging data via Structure-from-Motion (SfM) algorithms;
- 2) 3D Gaussian Splatting: Anatomical structures are modeled using optimized 3D Gaussians, which allow for efficient representation of complex tissues;
- 3) Real-time rendering: A tile-based rasterization algorithm supports real-time rendering at 1080p, enabling interactive exploration of the anatomy.

Results. The system achieves real-time rendering for 1080p resolution, with training times ranging from 6 to 50 minutes depending on the complexity of the anatomical structures at the Nvidia 3080 graphical processing unit. The method improves the visualization of detailed regions, such as the brain and heart, and outperforms traditional mesh-based rendering in both realism and interactivity.

Conclusions. The application of 3D Gaussian Splatting in anatomy education significantly enhances real-time 3D visualization and interaction with anatomical models. It provides an immersive experience for students and professionals, facilitating a better understanding of complex structures and improving applications in surgical planning, research, and virtual reality-based anatomy training.

The impact of neuronal ion channels in epilepsy: a current overview

Groma Valerija¹, Naumovs Vladimirs², Skuja Sandra¹

¹*Institute of Anatomy and Anthropology, Rīga Stradiņš University, Latvia*

²*Rīga Stradiņš University, Latvia*

Objectives. Epileptic seizures arise from an imbalance between excitation and inhibition in neurons, driven by hyperexcitability and hypersynchrony. Neuronal excitability and synaptic transmission are heavily influenced by the distribution of voltage-dependent ion channels, which have unique functions. These channels are crucial for neuronal excitability as they generate the depolarizing sodium currents needed to initiate and propagate action potentials. This study aims to investigate the distribution of voltage-gated sodium channels in the brains of epileptic patients, an area that has been less explored compared to research on animal models.

Materials and methods. Data for this study was collected from public databases, primarily PubMed and Scopus, while a preliminary morphological assessment was conducted based on a pilot search performed within the framework of the PHOTOTHERAPORT project.

Results. Voltage-gated sodium channels consist of a core molecular complex with a principal pore-forming α subunit, which has nine isoforms, and accessory β subunits. The encoded proteins Nav1.1, Nav1.2, Nav1.3, and Nav1.6 are key in the initiation and propagation of action potentials and are linked to various forms of genetic epilepsy. In the central nervous system (CNS), these four α subunits show distinct temporal and spatial distributions. Nav1.1 becomes more abundant after birth, particularly in caudal CNS regions (e.g., colliculus, medulla pons). Nav1.2 is present throughout development, especially in rostral regions (e.g., cortex, hippocampus). Nav1.3 peaks at birth and decreases in adulthood, while Nav1.6 is widely expressed without regional preference. Additionally, α subunits have specific localization patterns: types I, III, and VI are found in neuronal cell bodies, while type II is concentrated along axons. β subunits are strongly expressed in the cerebellum, hippocampus, and spinal cord.

Conclusions. Voltage-gated sodium channels are central to neuronal excitability and are critical therapeutic targets, including sodium channel blockers, in the treatment of epilepsy.

Comparative study of sodium-dependent glucose co-transporters in kidneys in norm and in T-2 mycotoxicosis

Hussar Piret¹, Allmang Cristin², Popvska-Percinic Florina³,
Dūrītis Ilmārs⁴, Järveots Tõnu²

¹ *University of Tartu, Estonia*

² *Estonian University of Life Sciences, Estonia*

³ *Ss. Cyril & Methodius University in Skopje, North Macedonia*

⁴ *Latvian University of Agriculture, Latvia*

Objectives. Among mycotoxins T-2 toxin is the most toxic trichothecene. Toxins produced by T-2 increase susceptibility against infections, cause necrosis in digestive tract, and dystrophy in liver, kidney, heart, brain, and peripheral ganglia of vegetative nervous system. In poultry consumption of feed contaminated with T-2 reduces chickens' weight gain, egg production, and hatching ability.

As up to now there is lack of comparative studies about effect of T-2 mycotoxin on expression of glucose transporters in kidneys, aim of our experimental investigation was to study expression of sodium-dependent glucose co-transporters-1 (SGLT-1) and -2 (SGLT-2) in kidney tissue comparatively in healthy and T-2 toxicated broilers.

Materials and methods. Kidney material was collected from three 7-days-old healthy (control group) and three 7-days-old female broilers with T-2 toxicosis. For T-2 toxin group, starting from fourth day after hatching, application of T-2 toxin in dose of 0.250 mg/day/bird was compulsive for three consecutive days. Sacrifice of chicks was 24 hours after last toxin application; thereafter, material from kidney was removed. Specimen were fixed with 10% formalin, embedded into paraffin, slices 7 µm thick were cut, followed by immunohistochemical staining with polyclonal primary antibodies Rabbit anti-SGLUT-1 and Rabbit anti-SGLUT-2, according to manufacturers' guidelines (IHC kit, Abcam, UK).

Results. Results showed strong expression of SGLUT-1 and SGLT-2 in epithelial cells of renal proximal tubules in control group's chicken. In T-2 toxin group birds' expression of both studied antibodies was weaker, brush border membranes of proximal tubule's epithelial cells were irregular and damaged, shrinkage of cell volume and heterochromatin condensation in nuclei was noticed. No significant changes were observed in distal tubules and collecting ducts in T-2 toxin group birds' kidneys.

Conclusions. Weak expression of SGLUT-1 and SGLT-2 and morphological changes in T-2 toxin group birds' kidneys indicates to the damage of kidney tissue and reduced glucose transport in urinary system during T-2 mycotoxicosis.

Insights for the usage of rats, rabbits and pigs as animal models in the improvement of treatment methods for heart arrhythmia

Inokaitis Hermanas¹, Paužienė Neringa¹, Pauža Dainius Haroldas²

¹ *Institute of Anatomy, Lithuanian University of Health Sciences, Lithuania*

² *Institute of Anatomy, Faculty of Medicine, Lithuanian University of Health Sciences, Lithuania*

Objectives. The study was designed to assess essential neuroanatomical differences of the cardiac conductive systems (CCS) in rats, rabbits and pigs since disordered neural control of this system has a paramount role in the development of cardiac arrhythmias.

Materials and methods. Immunohistochemical staining for hyperpolarization activated cyclic nucleotide gated potassium channel 4 (HCN4), choline acetyltransferase (ChAT), neural nitric oxide synthase (nNOS), tyrosine hydroxylase (TH), substance P (SP) and calcitonin gene-related peptide (CGRP) was applied for the visualization of the nodes of CCS and its innervation.

Results. The distributional pattern of HCN4 cells in the sinoatrial (SAN) was similar in all species examined. The area of SAN extended from the anterior part of the right cranial (superior cava) veins downwards to the terminal groove and the caudal (inferior cava) vein (CV). In all species, this area was occupied by nerve fibres positive for all the applied neuronal markers. In the rat heart, ganglionic cells in the SAN were specially found. In the rabbit heart, the small number of epicardial ganglionic cells was also revealed. The pig SAN contained the neural plexus with numerous ganglia in the epicardium and between the CCS cells. In the examined rats and rabbits, there were no ganglionic cells in the area of the AV node, yet the pig AV node involved numerous solitary nerve cells and even small ganglia.

Conclusions. Although the innervation pattern, in general, was similar in the CCS of the examined species, there were discovered substantial differences in the rats and rabbits in comparison with pigs. Therefore, the discovered species-dependent fact must be taken into account using these three mammalian species with the above-mentioned proposes.

Shortening of the gestational age of newborns during 1995–2020 period: analysis of Lithuanian medical data of births

Jakimaviciene Egle Marija¹, Isakova Jelena², Stasiunas Augustinas³, Tutkuvienė Janina¹

¹ *Department of Anatomy, Histology and Anthropology, Institute of Biomedical Sciences, Faculty of Medicine, Vilnius University, Lithuania*

² *Health Information Centre, Institute of Hygiene, Lithuania*

³ *Faculty of Medicine, Vilnius University, Lithuania*

Objectives. Shortening the gestational age (GA) has been the subject of debate for more than a decade. The aim of this study was to analyse the changes in the GA of single, live, naturally born newborns in Lithuania over twenty-five years.

Materials and methods. Medical data of births (1995, 2003, 2013, 2020) were analysed. GA was calculated from the date of the last menstrual period. Cases with the history of Caesarean section and all types of labor induction were excluded.

Results. Data of 70 030 newborns were analysed (50.68% boys). Decrease of the mean GA was observed in boys from 39.71 weeks in 1995 to 39.36 weeks in 2020 (difference was 2.45 days) and in girls from 39.72 weeks in 1995 to 39.43 weeks in 2020 (difference was 2.03 days). The gradual decline continued in all analysed years, but the biggest difference was between 2013 and 2020. The distribution of births by GA week groups showed a significant shift to the left (the frequencies of births at 37th week increased by 2.2/1.09 % in boys/girls respectively, at 38th week – by 4.6/4.01 %, at 39th week – by 13.88/13.49 %. However, frequencies at 40th week decreased by 16.42/15.43 % in boys/girls respectively, at 41st week – by 2.97/2.08, at 42nd week – about 1 % in both sexes. One way ANOVA revealed significant decrease of GA in both sexes across maternal age and parity groups.

Conclusions. During the 1995–2020 period in Lithuania, the mean GA of singleton, naturally born, term newborns reliably decreased by 2.45 days in boys and 2.03 days – in girls. This decrease resulted from the left shift in the distributions of births according to GA. The possible reasons of this phenomenon will be discussed in the presentation.

Evaluation of TGFβ1, HGF, FGF-2, FGFR1 and apoptosis in placentas of various gestational ages

Junga Anna, Pilmane Māra

Institute of Anatomy and Anthropology, Rīga Stradiņš University, Latvia

Objectives. The growth and development of the fetus are determined by the interaction of the mother and the fetus through the placental interface during pregnancy. An evaluation of transforming growth factor beta (TGFβ1), hepatocyte growth factor (HGF), basic fibroblast growth factor (FGF-2), fibroblast growth factors receptor 1 (FGFR1) and programmed cell death in the human placenta, and their correlations with pregnancy time and pregnancy outcomes may not only provide a better understanding of the role of growth factors and apoptosis in human development, but may also be of clinical importance in reproductive medicine.

Materials and methods. The research material was obtained from 53 patients without systemic diseases. The study analyzed the immunohistochemical identification of TGFβ1, HGF, FGF-2, and FGFR1 in placentas at different gestational ages. The staining of placental apoptotic cells was processed by an in situ cell death detection kit and their relative distribution was assessed by a semiquantitative counting method.

Results. We found few (+) TGFβ1, moderate (++) FGF-2 and numerous (+++) HGF and FGFR1 positive structures. Apoptotic cells were found in all the placental samples of various gestational ages; in general, their amount decreased with advancing gestational age of the placenta ($p < 0.05$). Apoptosis affected different types of cells: cytotrophoblasts, syncytiotrophoblasts, extravillous trophoblasts, and cells of the extraembryonic mesoderm.

Conclusions. TGFβ1 and FGF-2 did not play an important role in the development of the placenta beyond 22nd week of pregnancy, while HGF and FGFR1 immunoreactive cells increased with advancing gestation, indicating that the placenta maturation (growth, proliferation) is evolving, especially in the third trimester. Apoptotic cells are characteristics of all post-delivery placentas of various gestational ages; their number decreases with advanced gestation, suggesting a change to other ways of cellular disposal.

Variations of the sensory nerves of the dorsal aspect of the forearm and hand

Kachlik David, Khadanovich Anhelina, Herma Tomas,
Benes Michal, Kaiser Radek

*Department of Anatomy, Second Faculty of Medicine,
Charles University, Czech Republic*

Objectives. The dorsal aspect of the forearm and hand is supplied by four sensory nerves: the superficial branch of the radial nerve, the lateral antebrachial cutaneous nerve, the dorsal branch of the ulnar nerve, and the posterior antebrachial cutaneous nerve. The first three nerves feature frequent neural communications, which prevalence is not well known and which can cause clinical consequences.

Materials and methods. In two series, 306 forearms of body donors of Czech origin, embalmed with classical formaldehyde method, have been meticulously dissected. Any neural communications have been traced.

Results. The communicating branches (incorrectly called “anastomoses”) are quite thin and often short, and it is necessary to search for them intentionally and dissect meticulously to avoid damaging. According to our results, communicating branches between the superficial branch of the radial nerve and the lateral antebrachial cutaneous nerve were found in 74% of cases, which suggests that a communicating branch between these nerves represents a kind of normality. In 28% of cases, we observed more than one communicating branch in the same hand. In the majority of cases, the donor branch was emanated by the lateral antebrachial cutaneous nerve, and the recipient branch was the third branch of the superficial branch of the radial nerve, which supplies the radial side of the thumb.

Conclusions. From a neurological perspective, it is essential to understand that communications between the nerves can alter their sensory distribution and the area nervinae. From a surgical point of view, injury to a mixed branch containing fibers from both nerves can lead to the development of a painful neuroma, whether the injury is iatrogenic or traumatic.

Enhancing anatomy course with “Anatamage” radiological images: modules and implementation strategies

Kažoka Dzintra, Pilmane Māra

*Department of Morphology, Institute of Anatomy and Anthropology,
Rīga Stradiņš University, Latvia*

Objectives. This study aimed to create high-quality educational radiological image modules for integration into human anatomy courses and develop strategies for their implementation.

Materials and methods. In 2024, at the Department of Morphology of Rīga Stradiņš University, a virtual dissection table “Anatamage” with high-resolution radiological images (X-rays, CT scans, MRI) was used. Two anatomy tutors selected a set of pictures for creating the components. Modules were developed in Latvian and English, integrating images with questions, scenarios, and explanations.

Results. Incorporating radiological images into an anatomy course involved essential steps to ensure seamless integration with the three prepared modules. The first module was dedicated to “Introduction to radiological anatomy,” covering radiological terminology, orientation and planes, and fundamental radiological techniques. The second module focused on the “Skeletal system,” presenting the radiographic anatomy of bones, joints, the identification of fractures by discerning different types and their radiological manifestations, and the exploration of bone pathologies by recognising common bone diseases and conditions through radiological imagery. The third module, titled “Muscular system,” utilised MRI imaging to examine muscle anatomy, pathology, and soft tissue injuries, explicitly emphasising the identification and comprehension of soft tissue injuries through radiological images. The second and third modules encompassed normal (identification) and pathological topics (fractures, dislocations, tears, abnormalities, deformities, tumours, injuries) observed in X-rays, CT scans, and MRIs. Various strategies were employed to integrate radiological images into the anatomy course seamlessly and included interdisciplinary collaboration, enabling close cooperation with radiologists, anatomists, and educational technologists to devise comprehensive modules. Furthermore, provision was made for training tutors and students to acquaint them with the Anatamage Table and other radiological tools, developing interactive activities involving radiological images, implementing assessment and feedback mechanisms, and managing radiological image resources.

Conclusions. Created modules provide high-resolution and interactive visuals. Integrating radiological images into anatomy courses enhances diagnostic and clinical skills, bridging theoretical knowledge and practical application.

The association of neutrophil-to-lymphocyte ratio with in-hospital mortality in COVID-19 patients

Merkurjeva Kristine, Vidusa Liga, Štrumfs Boriss,
Uļjanovs Romans, Štrumfa Ilze

Department of Pathology, Rīga Stradiņš University, Latvia

Objectives. The global outbreak of COVID-19, triggered by Severe Acute Respiratory Syndrome Coronavirus 2 (SARS-CoV-2), caused one of the deadliest pandemics in the recent history, placing extraordinary demands on the health care system and its logistics. Cheap, widely available and easy-to-use tools would be helpful to estimate the severity of the clinical course of COVID-19 and thus plan the treatment. Paralleling morphological research of COVID-induced lung damage and the pathogenetic role of neutrophils, not limited to purulent superinfections, several studies have highlighted the importance of neutrophil-to-lymphocyte ratio (NLR) in COVID-19 cases. The aim of our study was to detect the prognostic importance of NLR in hospital-treated local COVID-19 patients.

Materials and methods. The study was performed as a retrospective evaluation of demographic data and NLR in patients, diagnosed with COVID-19 (by real time reverse transcription polymerase chain reaction) and undergoing treatment in a single university hospital. Based on the disease outcome within the hospital stay, the cases were classified as survivors (48) versus non-survivors (46).

Results. On admission, the mean NLR in surviving patients was $7.25 \pm$ standard deviation 4.18 [95% confidence interval: 6.04–8.47], ranging from 0.79 to 21.33. In contrast, the patients, who died during hospital stay, on admission presented with the mean NLR of 15.10 ± 18.05 [9.74–20.46]; range 0.43–116.5. By two-tailed Mann–Whitney test, the NLR difference between survivors and non-survivors was significant ($p = 0.001$). Both groups also showed statistically significant age difference: the mean age of survivors was 56.98 years [53.55–60.41], range 32–81; while the mean age of non-survivors was 70.17 [66.72–73.62], range 39–99 years. In non-survivors, NLR statistically significantly correlated with age (Spearman's $r = 0.29$; $p = 0.047$). In survivors, this correlation lacked statistical significance ($p = 0.306$). Both groups did not differ by the proportion of vaccinated patients and gender composition.

Conclusions. Higher NLR on admission and older age are associated with higher mortality in hospitalized COVID-19 patients.

Cardiovascular paleopathology in Lithuanian historical populations: evidence from mummified and skeletal remains

Mialkowskyj Damian, Jankauskas Rimantas, Kozakaitė Justina, Piombino-Mascoli Dario

*Department of Anatomy, Histology and Anthropology, Institute of Biomedical Sciences,
Faculty of Medicine, Vilnius University, Lithuania*

Objectives. This review aims to examine the prevalence of cardiovascular diseases in historical Lithuanian populations by analyzing published literature on mummified and skeletonized remains from the 17th to 19th centuries AD. Additionally, it seeks to understand the influence of genetic predispositions and environmental factors, such as diet and physical activity, on the development of cardiovascular diseases in these populations.

Materials and methods. The study focuses on mummified and skeletonized remains from crypts and subterranean chambers in Vilnius and Kėdainiai. Imaging of the mummified bodies was previously used to detect atherosclerotic changes, and further analysis of skeletal remains was conducted to identify evidence of cardiovascular pathology. Paleopathological, historical, and biomedical data were integrated to provide insights into cardiovascular diseases in these populations.

Results. Imaging revealed significant atherosclerotic changes in three adult mummies from Vilnius, suggesting that atherosclerosis was common among affluent individuals. Advanced cardiovascular pathology, such as aortic calcification and extensive calcification in the aorta, aortic valve, coronary arteries, and abdominal region, was observed in two mummified individuals from Kėdainiai. Additionally, skeletal evidence of an aortic aneurysm, including bone remodeling and sternal erosion, was identified in a high-status individual from the same site.

Conclusions. The findings suggest that lifestyle factors, such as diets rich in saturated fats and low levels of physical activity, contributed to the development of atherosclerosis, reflecting patterns observed in other ancient populations. Cardiovascular diseases like atherosclerosis and aortic aneurysms existed long before modern risk factors emerged. The integration of paleopathological, historical, and biomedical data emphasizes the role of both genetic predispositions and lifestyle in the development of cardiovascular diseases. Future research should focus on expanding sample sizes and incorporating genetic analyses to better understand the prevalence and etiology of cardiovascular diseases in the past.

Comparison of body mass index, body image and self-esteem among women aged 25–65 before COVID-19, during the first and second quarantine in Lithuania

Misiute Agne, Tutkuvienė Janina, Nedzinskiene Laura

*Department of Anatomy, Histology and Anthropology, Institute of Biomedical Sciences,
Faculty of Medicine, Vilnius University, Lithuania*

Objectives. Research on the impact of the COVID-19 pandemic on physical and psychological health, particularly body mass index (BMI), body image, and self-esteem, remains limited. This study aimed to fill this gap by assessing changes in these factors among women aged 25–65 in Lithuania during three periods: pre-pandemic, the first quarantine (March 16 – June 16, 2020), and the second quarantine (November 7, 2020 – June 30, 2021).

Materials and methods. A cross-sectional online survey was conducted in Lithuania with 796 women aged 25–65. Participants self-reported their weight and height for BMI calculation, categorized using WHO cutoffs (BMI ≥ 30 for obesity, 25.0–29.9 for overweight, ≤ 18.5 for underweight). BMI and body image were assessed across all three periods. Body image was measured using the Stunkard Figure Rating Scale (1965), where participants selected figures representing their current and ideal body size, with the difference indicating dissatisfaction. Self-esteem, measured during the second quarantine, was assessed using the Rosenberg Self-Esteem Scale (1965), which includes 10 self-worth statements scored from 0 to 30, with higher scores indicating greater self-esteem.

Results. BMI increased by less than 1 unit during both quarantines compared to pre-pandemic, with changes statistically insignificant ($p > 0.05$). Younger women had a mean BMI of ~ 24 , while older women averaged ~ 27 . Body dissatisfaction, according to the Stunkard Scale, rose significantly ($p < 0.001$), particularly among overweight and obese women. Self-esteem, measured during the second quarantine, averaged 20.88. There were no statistically significant correlations between BMI and self-esteem ($p > 0.05$).

Conclusions. Despite minor BMI increases over the three periods, body dissatisfaction rose significantly, especially among overweight and obese women. Although self-esteem remained stable for most, the growing dissatisfaction with body image may have long-term psychological effects, suggesting the need for targeted interventions to address body image concerns and mental health during prolonged societal restrictions.

Characterization of tissue immunity defense factors of the lip in primary dentition children with Bilateral Cleft Lip Palate

Ozola Laura, Pilmane Māra

Institute of Anatomy and Anthropology, Rīga Stradiņš University, Latvia

Objectives. Bilateral cleft lip and palate (BCLP) is one of the most common and severe orofacial multifactorial birth defects. The defect presents with various functional disturbances, including chronic inflammation. Immunity defense factors modulate immune response, inflammation, and healing of the tissues; therefore, they are vital in the assessment of the immunological status of the patient and in the understanding of morphopathogenesis and characteristics of BCLP. The aim was to assess the distribution of Gal-10, CD-163, IL-4, IL-6, IL-10, HBD-2, HBD-3, and HBD-4 in BCLP-affected tissue of primary dentition age children.

Materials and methods. Tissues were obtained from 5 patients (4 boys and 1 girl, 4–17 months old) during cheiloplasty. 5 controls were used for comparison. Immunohistochemistry, light microscopy, semi-quantitative evaluation and non-parametric statistical analysis were used to evaluate the tissue factors in patients and controls, as well as evaluate the statistically significant differences between the groups.

Results. A statistically significant increase of HBD-2, HBD-3, and HBD-4 positive structures was found in lip skin and mucosal epithelium, hair follicles, and blood vessels of patients. Notable increase was also noted in IL-4, IL-6, and IL-10 in the mucosal epithelium and CD163 in blood vessels. The connective tissue of patients presented with statistically significant decrease of Gal-10, IL-10, and HBD-3. Spearman's rank correlation revealed multiple significant correlations between all the factors observed.

Conclusions. The increase of human beta defensins indicate the formation of a line of defense to regain tissue homeostasis in chronically inflamed tissue. Upregulation of CD163 positive cells, increase of IL-4, IL-10, and decrease of Gal-10 points out the suppression of excessive damage from inflammatory reactions. A decrease of HBD-3, IL-10 in the connective tissue and an increase of IL-6 suggest decreased tissue healing, excessive scarring, and impaired protection against pathogens. The presence of various mutual correlations between the factors indicates mutually linked effects.

Facial cleft basic research in Latvia: search for the best methods and directions

Pilmane Māra

Institute of Anatomy and Anthropology, Rīga Stradiņš University, Latvia

Objectives. Facial clefts belong to the 2nd most common anomaly of the world with multifactorial aetiology. The main directions of our 20-year-long research was the detection of cytokine expression, antimicrobial protection and gene evaluation in the cleft lip palate (CLP).

Materials and methods. 20 primary dentition CLP lip were obtained for detection of IFN- γ , TNF- α , IL-2,7, 12, and IL-13; 8 palate of mixed dentition – for detection of HBD-2,-3,-4, LL-37, IL-10, and CD-163 - by IMH; 12 primary dentition CLP lip were evaluated for IL-2,4,5,6,10,12,13,17A, TNF- α , IFN- γ , TGF β -1 and GCSF by ELISA, and 27 lip/palate were searched for genes FGFR1,2, FOXO1, FOXE1, PAX7,9, SHH, SOX3, WNT3A,9B by CISH method.

Results. TNF- α , IL-2, and IL-12 were higher in the CLP epithelium. IFN- γ displayed minor immunoreactivity. A significant difference between study groups was observed for HBD-2 and IL-10. The number of HBD-3 cells was moderate in CLP, but LL-37 cells varied in both study groups, whilst CD-163 marked a moderate number of macrophages in patients. Numerous correlations between factors were revealed in CLP. From concentration, a significantly positive correlation was found between IL-2 and IFN- γ coupled with an IL4/IFN- γ ratio favoring IFN- γ . A reduction in TGF β -1 levels was noted. IL-6 was more highly correlated to IFN- γ and IL-12. FGFR1, FOXE1 were elevated in epithelium, and over-amplification of FGFR2 along with bFGF was observed.

Conclusions. The CLP affected epithelium displays high plasticity in expressing of cytokines. The increase in HBD-2, -4, and IL-10 suggests a compensatory elevation of the local immunity. A reduction in TGF β -1 levels contributes to mucosal damage. IL-6 correlation to IFN- γ and IL-12 indicates its proinflammatory role. FGFR1 indicates the cellular proliferation, local inflammation, and fibrosis, but FGFR2/bFGF promote the angiogenesis. Changes in CLP palatine epithelium seem to be influenced by PAX7 gene. The various correlations reflect the interactions of the gene-regulated pathways in postnatal CLP morphopathogenesis.

Understanding the impact of chronic hypertension on cardiac autonomic innervation from the end of life perspective

Ranceviene Dalia, Rysevaite-Kyguoliene Kristina,
Sabeckis Ignas, Paužienė Neringa

*Institute of Anatomy, Faculty of Medicine, Lithuanian University of
Health Sciences, Lithuania*

Objectives. Arterial hypertension (AH) is a silent killer – one of the predictor factors of mortality from cardiovascular disease. The objective of this study is to investigate intrinsic cardiac nervous system (ICNS) elements adaptation to chronic untreated AH at the end-of-life stage.

Materials and methods. Spontaneously hypertensive rat (SHR) model: three hypertensive and three normotensive male (> 18 months) rats. Three key ICNS limbs were assessed using immunohistochemical labeling on atrial and ventricular whole mounts and cryosections to quantify the density and distribution of sympathetic (adrenergic – tyrosine hydroxylase (TH+), parasympathetic (cholinergic – choline acetyltransferase (ChAT+)) and sensory (peptidergic – calcitonin gene-related product (CGRP+)) nervous structures. The results indicated a significant difference with p-value of < 0.05.

Results. The epicardiac ganglii conglomerates, exceptionally cholinergic, were unusually covered with connective tissue. The size of SHR neurons was lower. Epicardiac nerves were mixed, containing all three compartments.

We noticed an increase in the percentage of TH+ NF in the epicardiac nerves of the atria (+20%) and ventricles (+16%), as well as NF meshwork on the sinoatrial node (SAN) (+36%) and ventricular myocardium (+316%), but no difference in atrial myocardium.

The percentage of ChAT+ nerve fibers (NF) increased only in the atrial epicardiac nerves (+19%) and in the sinoatrial node (+180%), with no differences observed in the ventricles and other atrial regions.

While the amount of CGRP+ NF was the lowest, its percentage increased the highest in comparison to the other neuromarkers. CGRP+ levels were approximately more than doubled in epicardiac nerves (atrial + 136%, ventricular +77%) in myocardial meshwork (SAN +450%, atria +150%, ventricles +162%).

Conclusions. These results indicate a trend towards slight activation of adrenergic, minimal – in cholinergic, and fairly impressive – in the peptidergic limb of ICNS, which was not recognized appropriately previously.

Nerve supply of aorta in rats

Rekke Kirsten, Rysevaite-Kyguoliene Kristina, Onashko Yulia,
Sabeckis Ignas, Pauža Dainius Haroldas, Khmel Olena

*Institute of Anatomy, Faculty of Medicine, Lithuanian University of
Health Sciences, Lithuania*

Objectives. The study aims to demonstrate the morphologic pattern of innervation in the aorta since these specific data have pivotal importance for understanding the mechanism of painless aneurysm development.

Materials and methods. The ascending, descending (thoracic and abdominal) aorta and aortic arch of ten rats were examined microscopically following the staining of their neural structures for general (acetylcholinesterase, AChE), sympathetic (tyrosine hydroxylase, TH), and sensory (calcitonin gene-related peptide, CGRP) axonal markers.

Results. The evident AChE(+) nerves linked the sympathetic trunk with the aorta wall. These tiny nerves derived from sympathetic ganglia accompany the intervertebral arteries up to their access to the aortic wall. In the ascending aorta, the TH(+) axons were most numerous in the adventitial layer and occupied 1.5% of the area, while the CGRP(+) – 0.2% only. In the aortic arch, adrenergic axons comprised 1.4% and CGRP(+) – 0.1%, respectively. In the descendent aorta, TH(+) axons covered 0.4% (thoracic part) and 1.1% (abdominal part) of the wall area, whereas CGRP(+) – 0.14% and 0.12%, respectively. The aortic wall in rats is supplied by 3–4 tiny nerves derived bilaterally from sympathetic trunk ganglia at the descending thoracic aorta. The average length of these nerves is 7 mm, and they exhibit sympathetic adrenergic and sympathetic afferent axons that extend to the aortic wall.

Conclusions. The results of this study demonstrate the sympathetic and sensory innervation within the aortic walls in rats and further studies are needed for confirmation of our findings in large experimental animals and humans. The revealed significant quantitative differences in axonal density and morphologic pattern of innervation in the specific part of the aorta suggest the hypothesis about possible different neural regulation and sensibility of the aneurysm development in distinct parts of the aorta.

Comparative anatomy of the epicardial ganglionated nerve plexus in two pig breeds

Saburkine Inga, Rysevaite-Kyguoliene Kristina, Ranceviene Dalia,
Rekke Kirsten, Paužienė Neringa, Khmel Olena, Pauža Dainius Haroldas

*Institute of Anatomy, Faculty of Medicine, Lithuanian University of
Health Sciences, Lithuania*

Objectives. The present study aimed to examine the distribution of the epicardial ganglionated neural plexus in the hearts of pigs and mini-pigs, highlighting the quantitative differences of this plexus in these popular experimental animals.

Materials and methods. The pressure-distended whole hearts from the eight adults mini-pigs and the five adult Landrace pigs were stained histochemically for acetylcholinesterase, and subsequently studied with a stereomicroscope.

Results. In the mini-pigs and Landrace pigs, the principal mediastinal nerves accessed the heart at the same sites: the sinuses of the right cranial and the left azygos vein, yet the tiny accessing nerves – close to the pulmonary veins. In mini-pigs, the accessing mediastinal cardiac nerves were persistently determined at the roots of the left coronary artery. Within the epicardium of the Landrace and mini-pigs, nerves proceeded into discrete atrial and ventricular areas by five neural routes, so-called subplexuses: (1) the left and (2) middle dorsal, (3) dorsal right atrial, (4) right ventral, and (5) the ventral left atrial ones. Although the heart weight in the Landrace pigs was significantly larger than in the mini-pigs, both the thickness of the epicardial nerves and the areas of the epicardial ganglia were not different in these breeds in most sites. Nevertheless, the accessing cardiac nerves at the right cranial vein and the postganglionated nerves on the dorsal left ventricle and dorsal right atrial region were, correspondingly significantly, thicker or thinner in mini-pigs ($p < 0.05$). Similarly, only the epicardial ganglia of the ventral right atrial subplexus were significantly ($p < 0.05$) less in mini pigs compared with Landrace ones.

Conclusions. In conclusion, the results of our study demonstrate the early and noteworthy alterations in heart neuroanatomy of the mini-pig compared with the Landrace breed. The discovered differences may impact the heart electrophysiology employing mini-pigs as animal models in the functional experiments.

Cartilage degradation and synovial inflammation in osteoarthritis progression: morphological and molecular analysis

Semenistaja Sofija¹, Sokolovska Lība², Studers Pēteris³,
Kadiša Anda⁴, Groma Valērija⁵, Skuja Sandra⁵

¹ *Department of Doctoral Studies, Rīga Stradiņš University, Latvia*

² *Institute of Microbiology and Virology, Rīga Stradiņš University, Latvia*

³ *Hospital of Traumatology and Orthopaedics, Rīga Stradiņš University, Latvia*

⁴ *Department of Internal diseases, Rīga Stradiņš University, Latvia*

⁵ *Institute of Anatomy and Anthropology, Rīga Stradiņš University, Latvia*

Objectives. Osteoarthritis (OA) is a whole joint disease, involving the interaction of cartilage remodeling and synovial membrane inflammation (synovitis), which arises secondary to cartilage degradation and sustains these alterations. Cellular damage disrupts the regulation of collagenous and non-collagenous proteins of the cartilage extracellular matrix (ECM). These changes are reflected in the synovial fluid concentrations of cartilage ECM proteins, such as C-terminal cross-linked telopeptides of type II collagen (CTX-II) and cartilage oligomeric matrix protein (COMP).

This study characterizes cartilage degradation and synovial inflammation through tissue morphology and molecular analysis to establish their relationship in OA progression.

Materials and methods. Twenty-five surgically obtained joint tissue samples were processed for light microscopy analysis. Cartilage degradation severity was assessed using the OARSI score; the severity of synovitis was analyzed according to the Krenn grading system. The presence of CTX-II and COMP proteins in the synovial fluid was measured using ELISA. Statistical data analysis was conducted using the SPSS 28.0.

Results. The median OARSI score was 4.0 (3.0; 4.5), indicating superficial cartilage zone delamination. Single cells predominated over cellular clusters: 60.00 (45.00; 84.00) and 26.00 (22.00; 48.00), respectively. Proteoglycan staining was 1.00 (1.00; 2.00), depicting low intensity. ECM edema negatively correlated with proteoglycan staining ($r = -0.445$; $p = 0.043$). Synovitis severity equaled 2 (1.0; 3.0), depicting low-grade synovitis. Synovitis positively correlated with cartilage degradation severity ($r = 0.434$; $p = 0.034$). Mean CTX-II and COMP levels in synovial fluid were 1.09 ng/ml (SD 0.538) and 1262 ng/ml (SD 339.47), respectively. Correlations were found between CTX-II and OA severity ($r = 0.525$; $p = 0.008$), and COMP and OA severity ($r = -0.464$; $p = 0.022$). COMP and synovitis showed a positive correlation ($r = 0.405$; $p = 0.050$).

Conclusions. The correlation between synovitis and cartilage degradation underscores the importance of interplay between joint compartments in OA. The identified correlations between OA severity and cartilage turnover proteins in synovial fluid suggest their potential as potential biomarkers for monitoring OA progression.

Dynamics of general size and shape of the craniofacial compartment, and its sexual differences in Lithuanian adolescents, taking into account the pubertal growth spurt

Stukaite-Ruibiene Egle, Tutkus Jonas, Gervickaite Simona,
Šimkūnaitė-Rizgelienė Renata, Barkus Arunas, Tutkuvienė Janina

*Department of Anatomy, Histology and Anthropology, Faculty of Medicine,
Vilnius University, Lithuania*

Objectives. Craniofacial studies play an important role in forensic facial identification. However, research on craniofacial changes associated with body growth remains limited. The aim of this study was to evaluate the dynamics of craniofacial growth and sexual differences associated with the pubertal growth spurt (PGS).

Materials and methods. A total of 683 girls and 692 boys (aged 10–20) were included in the study. Standard anthropometric methods (L. G. Farkas, 1994; H. Greil, 2003) were used to assess height, body mass index (BMI), head length (HL), head breadth (HB), head circumference (HC), bizygomatic (BzW) and bigonial (BgW) widths, physiognomic (PhyFH) and morphological (MorFH) facial height. Coefficients of sexual dimorphism (SDCs) were calculated (Borgognini Tarli and Repetto, 1986).

Results. In 10–20 age period, the height of girls/boys increased from 141.0/141.3 to 168.9/182.7 cm. For girls, height PGS was at 10–13 years, for boys – at 11–15 years. In both sexes, BMI PGS started 1–2 years after height PGS. For girls, MorFH and PhyFH grew mainly at 11–13 years ($p < 0.01$), for boys – at 10–11 and 13–14 years. BzW and BgW increased the most in girls aged 10–11 years ($p < 0.01$) and in boys aged 12–13 and 15–16 years. HL increased the most in 12–13-year-old girls, 10–11 and 15–16-year-old boys, HW – in 12–13-year-old girls, 12–13 and 15–16-year-old boys. Sexual dimorphism increased until age 16–17, peaking between 13–14 and 15–16 years.

Conclusions. There was one period of rapid increase in craniofacial parameters of girls and two – in boys. In girls, vertical and transverse parameters grew mostly at the first phase of height PGS; however, in boys – vertical parameters grew most at the beginning and the end of height PGS; in addition, their facial widths grew more closely with BMI PGS. Sexual dimorphism stabilized only at the end of the growth period.

Etiopathogenetic mechanisms of vocal nodules and Reinke's edema development and their morphopathological manifestations

Sumerags Dins¹, Pilmane Māra², Segliņa Gunta³

¹ *Cesu Klinika Hospital, Latvia*

² *Institute of Anatomy and Anthropology, Rīga Stradiņš University, Latvia*

³ *Department of Otorhinolaryngology, Rīga Stradiņš University, Latvia*

Objectives. Vocal nodules and Reinke's edema are common benign vocal fold diseases associated with vocal fold overuse, smoking, and other environmental factors. The precise etiopathogenetic mechanisms are not fully understood. Thus, our aim was to study proliferation, programmed cell death, inflammation, and ischemia markers to reveal complex cellular and tissue-level interactions contributing to the pathogenesis of these conditions.

Materials and methods. Vocal nodules were obtained from 10 females (aged between 17 and 56) and five Reinke's edema-affected vocal cords (58 to 71 years old). Controls were obtained from the vocal cords of seven cadavers (aged 40–70 years). Ki-67, PGP 9.5, IL-10, IL-1 α , EGFR, VEGF, and apoptosis were detected by the biotin-streptavidin immunohistochemistry.

Results. In the case of vocal nodules, a significant increase in proliferation markers (Ki-67), growth factors (EGFR), ischemia (VEGF), and inflammation (IL-1 α) have been observed. These findings indicate a persistent inflammatory and ischemic environment, leading to hyperplastic changes in the tissue. Simultaneously, the intensification of apoptosis and its strong correlation with proliferation and inflammation suggest complex interactions maintaining the formation of vocal nodules.

Studies on Reinke's edema reveal an intense proliferation of the surface epithelium, associated with chronic inflammatory processes due to smoking and other external factors. Increased IL-10 marker expression indicates a pronounced anti-inflammatory response, attempting to compensate for the epithelial damage caused by inflammation. Furthermore, higher IL-1 α and PGP 9.5 expression is associated with inflammation, proliferation, and tissue remodeling processes in Reinke's edema.

Conclusions. These studies suggest that developing vocal nodules and Reinke's edema in the vocal folds are linked to similar etiopathogenetic mechanisms, where inflammation, cellular growth, and ischemic changes dominate. Further analysis of these markers could provide new opportunities in diagnosing and treating these diseases, potentially leading to more targeted therapeutic approaches that address pathological processes at the cellular level.

Radiomorphometric assessment of posterior condylar canals in children at the age between 2 months and 14 years

Szeliga Stanisław, Drożdż Adrian

*Department of Descriptive and Clinical Anatomy,
The Medical University of Warsaw, Poland*

Objectives. The aim of this study was to perform radiomorphometric evaluation of posterior condylar canals (PCC) among children between 2 months and 14 years old, focusing on the anatomical variability of the channels.

Materials and methods. The analyses were retrospectively carried out on 100 CT scans of patients at the age of 2 months to 14 years. The scans were performed in the neurosurgical department for diagnostic purposes.

Following their identification, the PCCs were classified regarding their internal orifice position. We established 6 patterns of PCCs, according to previous studies: the groove for sigmoid sinus (SS), the jugular foramen (JF), the hypoglossal canal (HGC), the groove for occipital sinus (OSS), the groove for marginal sinus (MS) and the combined type (COM). The curvature of the PCCs was assessed in axial and sagittal planes. The width and height were measured in three positions. In the case of bilateral occurrence, the dominant side was determined according to mean diameters.

Results. We identified 83 (83%) cases of the PCCs' presence. In 48 (48%) cases, the PCC was present bilaterally, while in 35 (35%) unilaterally, giving 131 sides with present PCC overall. The SS, JF, HGC, OSS, MS and COM types were observed in 47 (35.9%), 60 (45.8%), 0 (0%), 0 (0%), 3 (2.3%) and 11 (8.4%) sides respectively. The curved pattern in the axial plane was found in 58 (52.7%) PCCs, while in the sagittal plane in 61 (55.5%). The mean height of the PCC was 2.57 mm \pm 0.73 mm, while the mean width of the PCC was 3.04 mm \pm 0.89 mm. The dominant side was to be right in 18 (33.3%) cases and left in 16 (37.5%) cases.

Conclusions. The posterior condylar canal is a significantly variable structure regarding its shape, size and internal orifice position pattern. A better understanding of its anatomy among paediatric patients may be crucial in preoperative planning.

Role of maternal undernutrition: comparison of histomorphological changes in visceral organs and retinas of two-generation rat offspring

Šimkūnaitė-Rizgeliėnė Renata¹, Laurinavičiūtė Guoda¹, Reivytytė Rosita², Virbauskytė Viktorija², Semenkováite Justina², Šlažaitė Gerda², Strelčenko Jekaterina², Vosyliūtė Rūta³, Žalgevičienė Violeta³, Čepulienė Ramunė³, Bartuškienė Violeta³, Tutkuvienė Janina³

¹Department of Anatomy, Histology and Anthropology, Faculty of Medicine, Vilnius University, Lithuania

²Faculty of Medicine, Vilnius University, Lithuania

³Department of Anatomy, Histology and Anthropology, Institute of Biomedical Sciences, Faculty of Medicine, Vilnius University, Lithuania

Objectives. This study aimed to evaluate the effects of maternal undernutrition on the histomorphology of the liver, pancreas, thyroid gland, and retina in first (F1) and second (F2) generation rat offspring.

Materials and methods. Two generations of offspring were studied. Mothers were either 50% food-restricted before pregnancy (1EG) or before and during pregnancy (2EG). The control group (CG), as well as the offspring, was fed normally. Paraffin sections of the pancreas, liver, thyroid gland, and retina were stained with H&E, histomorphological parameters were evaluated and measured using CellSens software. Cryosections of eyes were stained with glial fibrillary acidic protein, ionized calcium-binding adaptor molecule 1, and RNA-binding protein, macroglia, microglia, and ganglion cells were evaluated using a digital tool.

Results. More pronounced hepatic steatosis and ballooning were observed in both F1 and F2 offspring, with 1EG showing more severe steatosis and 2EG a higher ballooning index. These changes were less pronounced in F2.

An increase in exocrine pancreas vacuolization was detected in F1 male 2EG and F2 male 1EG compared to CG, with a significant decrease in F2 male 2EG. Female EGs showed increased vacuolization in F2 compared to F1. There was no significant change in the surface area of Langerhans islets, except for a size increase in F1 male 1EG.

Thyroid follicles were fewer in F1 compared to F2, with larger follicular areas and cell height in F1. Signs of fibrosis and inflammation were more evident in F1 offspring.

F2 of the nutritionally restricted groups showed greater photoreceptor layer atrophy, higher Müller cell activity, and more microglial cells. There was no clear influence on the ganglion cell layer.

Conclusions. Maternal undernutrition influences the histomorphology of offspring, with less pronounced changes in F2. Visceral organs may exhibit greater plasticity and adaptability, while the eyes appear more protected against maternal malnutrition effects.

Tumour microenvironment in solid and haematological malignancies

Štrumfa Ilze, Šinkarevs Staņislavs, Štrumfs Boriss, Sperga Māris

Department of Pathology, Rīga Stradiņš University, Latvia

Objectives. In the Western world, malignant tumours represent a significant healthcare challenge, ranking as the second or, in some countries, even the leading cause of mortality. While the features of neoplastic cells have been targeted by multiple studies, a more limited information is available on tumour microenvironment (TME), representing the non-neoplastic cells within the tumour, capable to support or suppress the progression of the tumour and its response to treatment. Thus, a thorough understanding of tumour microenvironment is necessary to study cancer pathogenesis, identify novel therapeutic targets, and consequently adjust pathology reports.

Materials and methods. A wide scope of methods has been employed to study TME. Transcriptomics benefits from large data arrays, while immunohistochemistry is widely accessible and allows to integrate cellular morphology with molecular features.

Results. TME comprises cellular and non-cellular components. Regarding the cells, cancer-associated fibroblasts, macrophages, neutrophils, myeloid-derived suppressor cells, mast cells, and different subtypes of lymphocytes are prominent. These cells ensure a rich, bidirectional network of biological interplay with neoplastic cells, as well as tumour stem cells; besides molecular signaling, ferroptosis can be involved. Cytokines, growth factors, non-coding RNAs, and extracellular stromal proteins participate in the signalling and/or hold prognostic significance. The TME components can either promote or inhibit tumour growth and significantly influence the reaction to treatment by limiting drug delivery or contributing to an immunosuppressive environment.

Conclusions. TME can influence both cancer pathogenesis and the efficacy of anti-cancer treatment, especially immunotherapy. TME must be studied in regard to tumour type, as important differences between haematological malignancies and solid tumours are observed. Microenvironmental subtyping is developing and has a potential to become as important as molecular sybtyping of certain cancers. Pathologists must be ready to expand the tumour diagnostic protocols with the corresponding information because it is significant for further cancer treatment development.

Modern light microscopy techniques: overcoming the diffraction limit

Štrumfs Boriss, Šinkarevs Staņislavs, Uljanovs Romans, Štrumfa Ilze

Department of Pathology, Rīga Stradiņš University, Latvia

Objectives. The light diffraction limits the resolution in conventional optical microscopy by the lateral distance between the studied objects that equals to a half of the wavelength of the applied light. For the conventional light microscope, the Abbe diffraction limit is 0.25 μm . However, morphological studies of the structures and objects smaller than Abbe's limit, e.g., viruses (100 nm) and complex molecules (10 nm), are crucially important for understanding the biological processes at the cellular and subcellular level. Traditionally, this was the domain of electron microscopy. Nevertheless, in comparison with light microscopy, electron microscopy has certain limitations, including complex sample preparation and the impossibility to perform observations in living systems.

Materials and methods. Since 1978 when Cremer et al. published the first confocal laser scanning microscopy approach, a series of both deterministic: stimulated emission depletion (STED) microscopy, ground state depletion (GSD) microscopy, reversible saturable optical fluorescence transition (RESOLFT) microscopy; and stochastic: spectral precision distance microscopy (SPDM), photo-activated localization microscopy (PALM), stochastic optical reconstruction microscopy (STORM) and other super-resolution light microscopy techniques have been developed. In 2014, the Nobel Prize in Chemistry was awarded to Betzig, Moerner and Hell for the development of super-resolution fluorescence microscopy, bringing optical microscopy into the nanometre scale.

Results. Today, a broad spectrum of such techniques allows to take a direct look into resolution beyond diffraction limit making possible a sub-cellular and molecular level morphological exploration of the different objects including living cells. This also includes single-molecule localization and tracking methods.

Conclusions. A short overview presented here demonstrates the most important examples of modern light microscopy techniques.

Dynamics in the eyes, nose and lips areas of Lithuanian men from 4 to 30 years of age in relation to the size and shape of the craniofacial complex

Tutkus Jonas, Gervickaite Simona, Barkus Arunas, Tutkuvienė Janina,
Šimkūnaitė-Rizgeliienė Renata

*Department of Anatomy, Histology and Anthropology, Faculty of Medicine,
Vilnius University, Lithuania*

Objectives. Craniofacial research has gained momentum over the past decade due to the rapid development of new facial analysis technologies. However, there is a lack of research on different facial features starting from preschool ages to adulthood. The purpose of this study is to evaluate the dynamics of male eyes, nose and lips parameters and their proportionality to craniofacial complex from 4 to 30 years.

Materials and methods. A total of 1165 males were examined using standard anthropometric methods (L. G. Farkas, 1994; H. Greil, 2003): eye fissure width (EyFissW), interpupillary distance (PuDist), inner (InEyW) and outer eye widths (OutEyW), nose width (NW) and height (NH), nasal depth (ND), nasal bridge length (NbrL), labial width (LaW). A total of 22 proportionality indices were calculated.

Results. The widths and heights of different facial features at the 4 years and their relative increases until the age of 30 years were as follows (mm/%): EyFissW - 26.5 mm / 15.9%, PuDist - 50.1 mm / 27.5%, InEyW - 29.0 mm / 9.1%, OutEyW - 82.0 mm / 17.3%, NW - 27.9 mm / 30.7%, LaW - 36.4 mm / 48.5%; NbrL - 15.3 mm / 82.7%, NH - 32.4 mm / 65.6%, ND - 27.3 mm / 49.9%. The analysis of 22 proportionality indices of the craniofacial complex revealed that in general: eye fissure width became relatively smaller (several fluctuations were detected during puberty); nose became relatively elongated, however, certain nasal widening happened close to 30 years; relative labial width has increased.

Conclusions. 1. Within age period of 4-30 years, the greatest relative increase was detected in all nasal parameters and lip width, while the least relative increase was characteristic to the eye area ($p < 0.001$). 2. Proportionality of the eyes, nose and lips areas within the craniofacial complex, had several fluctuations during the puberty (due to different growth rates of the upper, middle and lower facial parts). 3. A slight relative increase in the width of facial features was detected near the age of 30 years as well ($p < 0.05$).

Secular trend in general size and shape parameters of head and face of Lithuanian adolescents during 1965–2015 period

Tutkuvienė Janina¹, Gervickaite Simona¹, Tutkus Jonas¹, Stukaite-Ruibiene Egle¹, Barkus Arunas¹, Almonaitiene Ruta², Šimkūnaitė-Rizgeliene Renata¹

¹Department of Anatomy, Histology and Anthropology, Faculty of Medicine, Vilnius university, Lithuania

²Institute of Dentistry, Centre of Clinical Odontology, Faculty of Medicine, Vilnius university, Lithuania

Objectives. There is a lack of research on the secular trend of craniofacial parameters in the 21st century, as most recent studies use 2D or 3D facial image analysis and cannot be compared with previous studies. The aim of this study was to evaluate secular trends in the craniofacial size and shape parameters of Lithuanian adolescents since 1965.

Materials and methods. During 2010–2015, a total of 528 boys and 552 girls aged 10–18 were examined using standard anthropometric methods (Martin-Saller, 1957): head circumference (HC), head length (HL – in sagittal plane), head width (HW), morphological facial height (MorFH), facial width (FW). Cephalic index (CI = HW/HL × 100) and facial index (FI = MorFH / FW × 100) were calculated. Results were compared with similar data from 1965 and 1985 studies that used the same methods and instruments.

Results. During 1965–2015, craniofacial parameters changed as follows: (1) HC increased throughout the period in boys ($p < 0.01$), but not in girls; (2) HL increased in boys ($p < 0.001$) and girls ($p < 0.01$), but only during 1985–2015; (3) HW did not change, comparing 2015 and 1965 data, but in 1985 a decrease was observed ($p < 0.05$); (4) MorFH increased steadily throughout the period ($p < 0.001$); (5) FW has increased significantly, comparing 2015 and 1965, but in 1985 a significant decrease was observed ($p < 0.001$); (6) CI decreased in 1965–1985 ($p < 0.01$), and until 2015 did not change significantly; (7) FI increased during 1965–1985 ($p < 0.001$), and in 2015 decreased again to become very similar to FI in 1965 ($p > 0.05$).

Conclusions. Head width did not change significantly, while head sagittal elongation happened. Hence, the shape of the head changed from brachycephalic to mesocephalic (starting from 1985). The face was narrowest in 1985 (hyperleptoprosopic), and in 2015, it became wider again, even exceeding the facial width in 1965 (mesoprosopic or euryprosopic).

Hotspot pattern in parathyroid pathology: implications for pathogenesis and diagnostics

Uljanovs Romans, Vidusa Liga, Štrumfs Boriss,
Merkurjeva Kristine, Štrumfa Ilze

Department of Pathology, Rīga Stradiņš University, Latvia

Objectives. Diagnostics of hyperparathyroidism is based on laboratory and radiological investigations. However, pathological assessment of surgically removed glands can help to verify the diagnosis or to reach it in difficult and/or recurrent cases. The aim of our study was to evaluate immunohistochemical hotspot pattern in parathyroid pathology.

Materials and methods. The study was performed as a retrospective morphological and immunohistochemical evaluation of parathyroid glands that have been surgically removed according to clinical indications. Computer-assisted morphometry was applied, and the obtained data were subjected to statistical analysis, including descriptive statistics as well as Kruskal–Wallis and Mann–Whitney tests. To evaluate the hotspot pattern, the clustering of cells was assessed both qualitatively (present/absent) and quantitatively by the difference of highest and lowest fraction (%) of positive cells. Differences were considered significant if $p < 0.05$.

Results. The difference between the highest and lowest fraction of positive cells was highest for cyclin D1, p21, and Ki-67, reaching up to 30.3%, 27.3% (both – in MPD), and 11.8% (in carcinoma), respectively. Qualitatively, these antigens showed a remarkable tendency to group in tight clusters of neighbouring positive cells. Both by morphological assessment of co-localisation and by statistical analysis, the clusters were not associated by innervation, assessed by the CD56-positive fibres; tumour/glandular microenvironment (extent of fibrosis, density of inflammatory cells) and stem cell differentiation in the parathyroid tissues by CD44 expression (all $p > 0.05$).

Conclusions. A remarkable hotspot pattern was observed in cell cycle activity, indicating on paracrine signalling in the pathogenesis of parathyroid disorders. Both by morphological assessment of co-localisation and by statistical analysis, the clusters were not associated by density of innervation, other features of the tumour/ gland microenvironment and parenchymal stem cell differentiation.

Investigation of genes and gene proteins in cleft affected tissue

Vaivads Mārtiņš¹, Akota Ilze², Pilmane Māra¹

¹*Department of Morphology, Institute of Anatomy and Anthropology,
Rīga Stradiņš University, Latvia*

²*Department of Oral and Maxillofacial Surgery and Oral Medicine,
Rīga Stradiņš University, Latvia*

Objectives. Craniofacial cleft morphopathogenesis is relatively unclear. It has been associated with cleft candidate genes which encode proteins that regulate facial tissue formation and differentiation but the distribution of these proteins in cleft affected tissue and interactions between them have not been well documented. The main aim of this study was to evaluate and compare the presence of cleft candidate gene coded protein containing cells within different cleft tissue types.

Materials and methods. Cleft tissue was arranged into 3 groups – unilateral cleft lip (UCL) with 36 patients, bilateral cleft lip (BCL) with 13 patients, cleft palate tissue (CP) with 26 patients. Oral mucosa tissue was obtained during cleft correcting surgery. Control groups were formed from patients without clefts (7 patients who had upper lip frenulum plastic surgery and 5 patients from the historical collection of the Institute of Anatomy and Anthropology of Rīga Stradiņš University). Immunohistochemistry was implemented to detect BarH-like Homeobox 1 (BARX1), Distal-less Homeobox 4 (DLX4), Forkhead Box E1 (FOXE1), Homeobox B3 (HOXB3), Muscle Segment Homeobox 2 (MSX2), Paired Box Transcription Factor 7 (PAX7) and 9 (PAX9), Receptor-like Tyrosine Kinase (RYK), Sonic Hedgehog (SHH), SRY-box Transcription Factor 3 (SOX3), Wntless-type MMTV Integration Site Protein 3A (WNT3A) and 9B (WNT9B) positive cells.

Results. Cleft candidate gene protein containing cells were detected in all patient and control groups with different distributions. Multiple statistically notable correlations were found between the evaluated proteins.

Conclusions. Healthy oral cavity tissue is characterized by WNT9B, WNT3A, and SOX3 being the most prominent, in moderate number – SHH, PAX7, HOXB3, FOXE1, practically no presence of BARX1 and MSX2 containing cells. UCL is characterized by the increase of BARX1, FOXE1, HOXB3 and PAX7; BCL – by the increase in DLX4, PAX9, and a decrease in SHH. All cleft phenotypes, including CP, had increased MSX2 and RYK and decreased SOX3, WNT3A, WNT9B in tissue.

Research ethics of morphological studies

Vētra Jānis

*Institute of Anatomy and Anthropology, Department of Anthropology,
Rīga Stradiņš University, Latvia*

Objectives. This study aims to analyze the application of the Research Ethics principles and regulatory framework specifically regarding research conducted in morphology-anatomy, histology, pathology, embryology.

Materials and methods. Legislative sources, RSU documents, RSU Research Ethics Committee documents

Results. This study analyzes data from January 2021 to August 2024. During the mentioned time period, the RSU Research Ethics Committee (REC) has received 2,635 submissions for consideration. In morphology, there have been a total of 11 submissions throughout this period.

The activity of submissions to the REC does not reflect the actual activity in the field of morphology. Examining this situation reveals several problem areas. Morphological studies often take place over a long period of time, therefore ethical opinions have been issued many years ago and often no longer correspond to current regulatory framework and practice. Research is carried out within the framework of cooperation projects, in which research ethics permits have been issued in other countries, but the tissue material is taken in Latvia. Blocks with fixed tissues are located in university archives, but the information about the origin of the tissues can be interpreted in accordance with the requirements of current regulatory acts. General Data Protection Regulation (GDPR), the Law on the Rights of Patients, and several other regulations create legal barriers to the long-term storage of tissue samples.

Conclusions. Research ethics regulation remains incompletely aligned with morphology research practice and public health interests.

Endotypes of chronic rhinosinusitis with primary and recurring nasal polyps in the Latvian population

Vīksne Rūdolfs Jānis¹, Segliņa Gunta², Pilmane Māra³

¹*Rīga Stradiņš University, Latvia*

²*Department of Otorhinolaryngology, Rīga Stradiņš University, Latvia*

³*Institute of Anatomy and Anthropology, Rīga Stradiņš University, Latvia*

Objectives. Chronic rhinosinusitis (CRS) is a complex syndrome with various inflammatory mechanisms resulting in different patterns of inflammation that correlate with the clinical phenotypes of CRS. Our aim was to use detected IL-1, IL-4, IL-6, IL-7, IL-8, IL-10, IL-12, Ki 67, HBD-2, HBD-3, and LL-37 to classify specific inflammatory endotypes in chronic rhinosinusitis with the tissue of nasal polyps (CRSwNP).

Materials and methods. Samples from 35 individuals with primary and recurrent CRSwNP were taken during surgery. The tissues were stained for the previously mentioned biomarkers immunohistochemically. A hierarchical cluster analysis was performed. The clinical parameters were compared between clusters.

Results. Five clusters had significantly different biomarkers between groups. There were no significant differences in the clinical parameters, except for the Lund–Mackay score, which was significantly higher in cluster 4 compared to that of cluster 1 ($p = 0.024$). Five endotypes of (CRSwNP) are characterized by different combinations of type 1, type 2, and type 3 tissue inflammation patterns.

Conclusions. In the Latvian population, endotypes associated with neutrophilic inflammation or a combination of neutrophilic inflammation and type 2 inflammation are predominant. Increased proliferation marker Ki 67 values are not associated with more severe inflammation in the tissue samples of chronic rhinosinusitis with nasal polyps.

Evaluation of immunomodulatory tissue factors in gallbladders of pediatric patients with calculous cholecystitis

Zariņa Kaiva Zīle¹, Pētersons Aigars¹, Pilmane Māra²

¹ Rīga Stradiņš University, Latvia

² Institute of Anatomy and Anthropology, Rīga Stradiņš University, Latvia

Objectives. The increasing incidence of gallstones and cholecystectomy in pediatric populations highlights the growing concern over chronic cholecystitis, however, the morphopathogenesis of pediatric calculous cholecystitis remains underexplored. The aim of this study was to determine the expression and distribution of interleukin-12 (IL-12), interleukin-13 (IL-13), interleukin-1 β (IL-1 β), sonic hedgehog protein (SHH), nuclear factor NF-kappa-B p65 subunit (NFkBp65) and heat shock protein 60 (HSP60) in the gallbladder wall.

Materials and methods. Eleven gallbladder samples were obtained from pediatric patients with calculous cholecystitis during surgery. Five healthy gallbladder samples were used for controls. IL-12, IL-13, IL-1 β , SHH, NFkBp65 and HSP60 were detected by immunohistochemistry. The number of positive structures in gallbladder epithelium, blood vessels, and inflammatory infiltrate was counted semi-quantitatively by microscopy. Mann-Whitney U test and Spearman's rank-order correlation coefficient was calculated.

Results. SHH, NFkBp65, and HSP60 positive cells dominated in the epithelium of patients, but interleukins were moderately expressed in both – epitheliocytes and blood vessels of patients. Inflammatory cells displayed all interleukins, HSP60, and NFkBp65 positivity. Interestingly, IL-1 β showed more positive epitheliocytes in controls. Statistically significant differences between patient and control samples were seen in the expression of IL-1 β , SHH, NFkBp65 in epithelium, and in the expression of IL-12, SHH, and HSP60 in blood vessels. Very strong positive correlation was seen between the expression of IL-1 β and SHH in inflammatory infiltrate ($r_s = 0.921$, $p < 0.001$). Strong positive correlation ($r_s = 0.7-0.9$) was seen between IL-13 and SHH, IL-13 and HSP, IL-13 and NFkBp65, IL-13 and HSP60, IL-12 and NFkBp65, IL-1 β and NFkBp65, SHH and NFkBp65.

Conclusions. An increased number of NFkBp65, IL-12 and HSP60 positive cells suggest a significant role of immunomodulation in the pathogenesis of the disease. The notable expression of SHH in patient gallbladder tissue indicates its part in tissue regeneration and repair processes in calculous cholecystitis. The strong positive correlations between studied factors reveal the importance of their coordinated action in the morphopathogenesis of calculous cholecystitis.

A case study on the pulmonary arterial tree: detailed anatomical and topographical analysis

Zicāns Matīss¹, Kažoka Dzintra², Skride Andris³, Pilmane Māra²

¹ *Rīga Stradiņš University, Latvia*

² *Institute of Anatomy and Anthropology, Rīga Stradiņš University, Latvia*

³ *Department of Internal diseases, Rīga Stradiņš University, Latvia*

Objectives. Extensive research is required to comprehensively understand the complexity of the anatomy of pulmonary arteries and their branching for several invasive medical procedures. This study aimed to assess the branching of the right and left pulmonary arteries by measuring arterial branching angles, describing the course of each artery, and measuring morphological parameters such as length and diameter.

Materials and methods. The study utilized a preserved human cadaver from the Anatomy Laboratory at the Institute of Anatomy and Anthropology. The dissection focused on removing the lungs from the chest cavity. The procedure included cutting the bronchi, veins, and nerves while keeping the arteries intact up to the subsegmental level. The dissection tools used were a scalpel and surgical forceps. Measurements were taken using a digital caliper accurate to 0.01 mm and a 5° plastic protractor. Additionally, the study examined variations in the branching of pulmonary arteries and compared its findings with scientific literature from PubMed and Scopus.

Results. The lungs were carefully dissected for accurate measurements. The larger branches closer to the center of the lungs formed wider angles, almost reaching 90 degrees, while the angles of the smaller branches toward the outer areas ranged from 30 to 45 degrees. The diameter of the blood vessels decreased gradually from the main pulmonary artery to the outer edges of the lungs. However, the lengths of each branching artery did not follow a consistent decrease pattern. Additionally, each lung was found to contain ten segmental arteries, and the examination revealed unusual branching patterns.

Conclusions. The pulmonary arterial branching, course, and terminology of the two lungs exhibit distinct differences. Anatomical variations in each lung pose challenges for invasive procedures, requiring specialists to understand them comprehensively. Detailed anatomical knowledge supports the development of advanced medical technologies and techniques, ultimately contributing to better healthcare practices and patient care.



Poster presentations

Differences in expression of Defensin-3, Defensin-2, LL-37, Galectin-10, CD163 in oral mucosa of control group and patients with chronic periodontitis

Apele Zane, Pilmane Māra

Institute of Anatomy and Anthropology, Rīga Stradiņš University, Latvia

Objectives. The oral health status generally depends on the common health, other diseases and people's habits. Problems with oral mucosa usually start with changes of local immunity. The aim of the work was the determination of the local defence factors in periodontitis affected oral mucosa and the comparison of it with the healthy tissue.

Materials and methods. The chronic periodontitis group included patients after conservative periodontal treatment who had not reduced the depth of periodontal pockets and required surgical treatment to reduce them. The controls included patients who underwent clinical tooth crown lengthening surgery to improve esthetics for dental prosthetic purposes. Tissue was obtained from the gingival and dental sulcus. Gal-10, HBD-3, HBD-2, LL-37, and macrophage (M2-anti-inflammatory) receptor CD163 was detected by immunohistochemistry, data were evaluated semi-quantitatively with following statistical analysis (Mann-Whitney U test and Spearman's correlation test).

Results. The routine staining revealed moderate to prominent intra- and subepithelial infiltration without difference between the subject groups. A few to a moderate number of Gal-10, HBD-3, and HBD-2 positive cells were detected in all gingival samples in the controls, while LL-37 and CD163 marked only a few cells. Patient gingival samples showed few numbers of Gal-10, HBD-3, LL-37, HBD-2, and occasional CD163 positive cells. Spearman's rank correlation revealed one strong negative correlation in the patients between HBD-2 positive cells in the connective gingival tissue and HBD-3 in the epithelium of the gingiva. Mann-Whitney U test did not show statistically significant differences between the groups.

Conclusions. The gingival tissue of different places in the oral cavity demonstrate chronic inflammation, what seems characteristic for both - periodontitis and healthy subjects, suggesting the non-satisfactory status of oral mucosa in part of Latvian people. This is also proved by the lack of statistically significant differences in the expression of Defensin-3, Defensin-2, LL-37, Galectin-10, CD163 positive cells between the controls and patients.

Analysis of arm span to height ratio in Latvian residents from different regions based on 1930s data

Asare Lāsma¹, Vētra Jānis², Ivanovs Andrejs¹

¹ *Statistics Unit, Rīga Stradiņš University, Latvia*

² *Institute of Anatomy and Anthropology, Department of Anthropology, Rīga Stradiņš University, Latvia*

Objectives. This study aims to analyse the arm span to height ratio (ASHR) using data from the 1930s, collected from individuals in different regions of Latvia.

Materials and methods. Anthropological expeditions led by J. Primanis were conducted in Piebalga (1936), Jurmala of Vidzeme (1937), and the Zemgale district (1939). These included measurements of arm span and height. A person's arm span is the distance from the left hand's middle fingertip to the right hand's middle fingertip when stretching out both arms horizontally. The ASHR was calculated by dividing arm span by height, both measured in centimetres. A total of 6,324 adults were analysed.

The median and interquartile range (IQR) described non-normally distributed variables. Data were analysed using IBM SPSS Statistics 29.0.

Results. The study included 2,733 males (43.2%) and 3,591 females (56.8%). The median ASHR for males was 1.05 (IQR: 1.03–1.07) in Zemgale and 1.06 (IQR: 1.04–1.08) in both Jurmala of Vidzeme and Piebalga. For females, the median was 1.03 (IQR: 1.01–1.05) in Zemgale and 1.05 (IQR: 1.03–1.06 and 1.03–1.07) in Jurmala of Vidzeme and Piebalga, respectively.

The Kruskal-Wallis test showed statistically significant differences in ASHR between the regions for both genders ($p < 0.001$). Pairwise comparisons found significant differences between Zemgale and Jurmala of Vidzeme ($p < 0.001$) and between Zemgale and Piebalga ($p < 0.001$).

Conclusions. The arm span to height ratio reveals significant differences in body structure among Latvian residents across regions during the 1930s.

Mastering epoxy resin for educational model creation

Bode Mārtiņš¹, Strance Ģertrūde¹, Kažoka Dzintra²

¹ *Faculty of Medicine, Rīga Stradiņš University, Latvia*

² *Institute of Anatomy and Anthropology, Rīga Stradiņš University, Latvia*

Objectives. The study aims to conduct a literature review on preservation methods and associated complications to achieve successful organ preservation using epoxy resin and establish a relationship between the volume of air in the organs and the requisite maximum quantity of epoxy resin for adequate preservation.

Materials and methods. The specimens underwent a sequential immersion process for preservation and preparation. Initially, they were placed in a 95% ethanol solution for 24 hours to disinfect and remove excess fat, thus preventing interference with subsequent epoxy resin hardening. A 1 : 1 solution of glycerol and 95% ethanol was used for 12 hours to preserve the original color and structure. Subsequently, the specimens were immersed in 95% ethanol for 10 minutes to eliminate any residual glycerol, which could impede the application of textile acrylic colors before scaffold placement and epoxy resin pouring. Upon resin hardening, the specimens were sanded with sandpaper and then coated with dispersion varnish to ensure durability and optical clarity.

Results. The accepted theory was that a considerable quantity of air was present within the organs. To accomplish the intended goal, the procedure involved carefully applying layers of epoxy resin followed by using a vacuum chamber to extract any air that may be trapped within the material. This method was highly effective in preventing the formation of bubbles and cracking. Additionally, it was essential to color the main structures of the organs appropriately, as the epoxy resin didn't seamlessly blend with fabric colors when preserving the organs.

Conclusions. The varying air content of individual organs necessitates careful consideration of the volume of epoxy resin suitable for a single layer when producing an educational model. Utilizing vacuum and material refinement is imperative to achieve optimal quality outcomes. This approach offers notable advantages over formaldehyde in academic applications, including eliminating the necessity for gloves and masks during model manipulation.

Characterization of the pro-inflammatory, regulatory and anti-inflammatory cytokines of placenta in different gestation times

Brikune Elizabete, Pilmane Māra

Institute of Anatomy and Anthropology, Rīga Stradiņš University, Latvia

Objectives. The maternal immune system must balance tolerance and defense to support the genetically distinct fetus during the pregnancy. Recent declines in successful pregnancies and births have increased interest in understanding the role of placental function in these outcomes. This study explores how the regulatory, inflammatory and anti-inflammatory cytokines change within the placental development.

Materials and methods. A cross-sectional analysis was performed on 15 placentas from pregnancies at 28, 31, and 40 weeks, all showing placental distress syndrome. The placentas were obtained from Rīga Stradiņš University AAI tissue archive, categorized according to WHO guidelines. Immunohistochemistry was used to detect cytokines IL-1 α , IL-2, IL-4, IL-6, IL-7, IL-8, and IL-10. The data were evaluated semi-quantitatively and with statistical methods: the Kruskal-Wallis Test and Spearman's rank correlation to identify significant differences and correlations.

Results. Different gestational time placentae demonstrated an abundance of Hofbauer cells, irregularly obliterated blood vessels and fibrinoid. IL-1 α was consistently expressed across all researched gestational stages. IL-7 increased significantly at 31 weeks but was less prominent at other stages. IL-2 and IL-8 positivity declined from 28 to 40 weeks, while IL-4 and IL-10 were only sporadically detected. IL-6 was selectively expressed, particularly in macrophages. Significant differences of the IL-4 and IL-2 positive structures of the cytotrophoblast, macrophages, and endothelium were seen across gestational ages, with correlations observed also between other cytokines and structures.

Conclusions. The main structures positive for the cytokines are macrophages, cytotrophoblast, and extraembryonic mesoderm in different gestation placentae. The dominant expression of IL-1 α throughout gestation underscores its vital role in placental function in the first defence line. IL-7's fluctuation and IL-6's selective presence indicates their stage-specific roles, while IL-4 and IL-10 appear to possess rather individual changes. IL-2 and IL-8 seem to play a role in 2nd trimester of pregnancy, with its decrease in the 3rd one.

Differences of tissue factors in bone and cartilage between first-time and re-operated patients affected by facial clefts

Buile Dace¹, Pilmane Māra², Akota Ilze³

¹ *Rīga Stradiņš University, Latvia*

² *Institute of Anatomy and Anthropology, Rīga Stradiņš University, Latvia*

³ *Department of Oral and Maxillofacial Surgery and Oral Medicine,
Rīga Stradiņš University, Latvia*

Objectives. Facial clefts are one of the most common congenital craniofacial pathologies. It is important to understand which tissue factors could affect the regeneration of tissues and their successful healing after first-time and repeated surgery.

Materials and methods. Relative number and distribution of tissue proteinases (MMP-2, MMP-8, MMP-9) and their inhibitors (TIMP-2), mineralization factors (OC, OPN), osteoclast genesis suppressor (OPG), growth factors (TGFβ1, BMP-2/4, bFGF), cytokines (IL-1α), tissue-protective factors (HBD-2, HBD-3, IL-10), gene proteins (Runx2, Wnt3a) and apoptotic cells were determined in bone and cartilage tissue for cleft patients and control group. The number of bones obtained from patients who underwent osteoplasty or rhinoplasty for the first time was 14. The number of bones from reoperated patients was 22. The number of cartilages from the surgeries where rhinoplasty was performed as the first surgery was 17. The number of cartilages obtained from rhinoplasty, performed as repeated surgery was 21. The relative amount of immunohistochemically positive osteocytes and chondrocytes was evaluated with a semi-quantitative counting method. Data were analyzed using the Mann-Whitney U test.

Results. A statistically significant difference in MMP-2 positive osteocytes and apoptosis-positive chondrocytes was found between first-time and re-operated cleft patients. MMP-2 presented with the majority in re-operated cleft patients ($U = 95.50$; $p = 0.05$). Apoptosis-positive chondrocytes were present in most first-time cleft patients ($U = 107.50$; $p = 0.021$). There were no statistically significant changes in other tissue factors.

Conclusions. In the bone tissue of repeatedly operated cleft patients, an increase in the number of MMP-2 indicates a selective action of MMP with the activation of the main cell MMP – MMP-2. The cartilage tissue of first-time operated cleft-affected patients reveals an increased number of positive structures of apoptosis as promotion of programmed cell death in case of surgical correction of tissues.

In-person and remote anatomy studies, application of digital tools in anatomy teaching: a comparative study

Čepuliene Ramune, Miliauskiene Zydrune, Tutkus Vytautas, Šimkūnaitė-Rizgeliene Renata, Vosyliute Ruta, Nedzinskiene Laura, Tutkuvienė Janina

*Department of Anatomy, Histology and Anthropology, Institute of Biomedical Sciences,
Faculty of Medicine, Vilnius University, Lithuania*

Objectives. During the COVID pandemic, anatomy studies were conducted remotely, teaching migrated into a virtual environment. Innovative teaching methods and modern digital tools were used. After the pandemic lectures remained remote, while practical work was conducted in-person. The aim of the study was to assess the past 5 years results of exams of Physical Therapy students comparing in-person and remote studies. The effect of applying modern digital tools was evaluated.

Materials and methods. Results of first semester exam of Functional Anatomy of Physical Therapy students for the 2019–2024 were obtained from database. During pandemic 2019–2022 active teaching methods encouraging critical thinking were applied. In 2022–2024 modern digital tools (Slido, Kahoot) were applied.

Results. During 2019, all assessments were done using open questions. The average score was 7.0, and 12% of students failed to pass exam. In 2020, teaching was remote, all assessments were closed type tests, the average exam score was 6.9 and 6.5% of students failed. In 2021 semi-contact teaching and open-ended questioning returned, the exam was test style from classroom. This resulted in the score increase of up to 7.8, ($p < 0.01$), and all students passed the exam. In 2022 assessments remained the same, however score decreased to 7.1 ($p < 0.01$) and 6% of students failed. In 2023, digital tools Slido, Kahoot used, oral quizzes with evaluations were introduced. Results of quizzes accounted for part of the final colloquium scores. The exam was a test based from classroom, and the average score was the same – 7.1 ($p < 0.01$), but none of the students had failed to pass the exam.

Conclusions. Return to in-person learning had positive impact on students' academic performance. The newly introduced modern methods and digital tools didn't have influence on the average exam score but had promoted consistent learning and reduced number of failures at exam.

Experimental comparative study of dichloroacetate salts and temozolomide effects on pediatric glioblastoma in vivo and in vitro

Damanskienė Eligija, Balnytė Ingrida, Valančiūtė Angelija, Stakišaitis Donatas

Lithuanian University of Health Sciences, Lithuania

Objectives. The study aimed to investigate the anticancer effectiveness of sodium dichloroacetate (NaDCA), magnesium dichloroacetate (MgDCA), and temozolomide (TMZ) on pediatric glioblastoma PBT24 (boy's) and SF8628 (girl's) cell xenograft in a chicken chorioallantoic membrane (CAM) model and in vitro.

Materials and methods. The study groups in the CAM model were: control, treated with 5 and 10 mM NaDCA, 2.5 and 5 mM MgDCA, and 50 μ M TMZ. Tumor growth, invasion frequency into CAM, and the number of blood vessels in CAM were assessed in H-E histological preparations. Survivin expression in tumors was evaluated by immunohistochemistry. The expression of the NKCC1 gene (SLC12A2) in cells treated with 3 mM NaDCA, 1.5 mM MgDCA, and 50 μ M TMZ was tested by RT-PGR.

Results. Compared to the corresponding control, the tumor invasion into CAM frequency was significantly reduced in 10 mM NaDCA and 5 mM MgDCA treated groups. The number of CAM blood vessels was significantly reduced in PBT24-5 mM MgDCA and PBT24-50 μ M TMZ tumors. Both NaDCA doses reduced neoangiogenesis in the SF8628 tumor. The 10 mM NaDCA reduced survivin expression in tumor tissue. 5 mM MgDCA reduced survivin expression only in the SF8628 tumor, but TMZ did not affect survivin expression. DCA treatment did not affect SLC12A2 expression in PBT24 and SF8628 cells. The SLC12A2 expression was significantly higher in 50 μ M TMZ-treated cells than in the control.

Conclusions. The efficacy of DCA treatment on PBT24 and SF8628 tumor invasion in CAM and survivin expression in tumors was dose-dependent and more effective than TMZ treatment. Differences in treatment effects on neoangiogenesis were found among PBT24 and SF8628 tumors. TMZ increased SLC12A2 expression, but this adverse effect was not mediated by DCA.

Growth factors in the wall of anomalies-affected gallbladder of children

Derbeneva Darja¹, Pilmane Māra², Pētersons Aigars¹

¹ Rīga Stradiņš University, Latvia

² Institute of Anatomy and Anthropology, Rīga Stradiņš University, Latvia

Objectives. Folded gallbladder or cystic duct cysts are connected to chronic inflammation and evacuation disorders. These are rare congenital deformations, occurring with an incidence of 0,15% in fetuses and 1% in adults; however, information on the pediatric population is missing. Morphopathogenesis is also unclear and enrolls possible involvement of genes, gene proteins and growth factors. Consequently, this study aims to discover the appearance, distribution, and interactions of gene proteins SHH, IHH, HOXB3 and growth factors/their receptors HGF, IGF1, IGF1R in the wall of folded gallbladder and cysts of the cystic duct in children.

Materials and methods. The gallbladder samples were obtained from six children aged from 6 to 18 years during cholecystectomies. For controls, five regular gallbladders were retrieved from car accident-perished children. The samples were immunohistochemically stained for SHH, IHH, HGF, IGF1, IGF1R, and HOXB3 and data were evaluated semi-quantitatively. Mann-Whitney U and Spearman's tests were used to determine statistically significant results.

Results. Decreased appearance of SHH, IHH, IGF1R, and an increased number of HOXB3 positive cells in patient material compared to controls was detected. A statistically significant difference between the patient and control gallbladder was observed: in the epithelium and connective tissue for SHH positive cells; for all tissues of IHH; for epithelium, blood vessels and smooth myocytes of IGF1R; for smooth myocytes of HOXB3 positive cells. However, the strongest positive correlations were found between epithelial IHH, SHH, and IGF1R, as well as between epithelial IGF1R and blood vessels.

Conclusions. The decrease of the main endodermal gene proteins SHH/IHH along with the diminished IGF1R positive cells suggests their possible involvement into the development of gallbladder anomalies. Additionally, HOXB3 increase for these conditions proves probably the stimulated growth properties, while the HGF and IGF1 seems not to be most important players in development of folded gallbladder and cystic duct cysts.

Lung cancer cell tumors respond differently to the treatment with sodium valproate in the chicken embryo chorioallantoic membrane model

Diržiuvienė Raminta, Šlekiene Lina, Palubinskienė Jolita, Balnytė Ingrida, Lasiene Kristina, Stakišaitis Donatas, Valančiūtė Angelija

*Department of Histology and Embryology, Faculty of Medicine,
Lithuanian University of Health Sciences, Lithuania*

Objectives. Lung cancer is the most frequent cause of cancer death. There are two main histological subtypes of lung cancer: non-small-cell lung cancer and small-cell lung cancer. Tumor progression is associated with increased vascularization. In our research, we tested the possible antiangiogenic and anti-migratory effect of valproic acid in experimental lung tumors grafted on the chicken embryo chorioallantoic membrane (CAM).

Materials and methods. The effect of different doses of sodium valproate (NaVP) on angiogenesis was tested, and quantification of CAM parameters such as blood vessel density and CAM thickness was performed. Experimental tumors, used for tumor progression and angiogenesis research in this study, were formed using 3 different lung cancer cell lines: A549, Sk_Lu_1, and NCI-H146. All cell lines formed tumors, which were treated with different doses of NaVP.

Results. Our results show that NaVP treatment induced a dose-dependent decrease of the experimental tumor invasion into the CAM mesenchyme and its angiogenic response. Both depend on the cell line: invasion and the angiogenic response of the tumors from A549 and NCI - H146 cell lines responded to the increasing doses from 4 to 8 mM of NaVP, whereas Sk_Lu_1 cells' response was antimigratory and antiangiogenic up to dose of 6 mM of NaVP. The dose of 8mM NaVP stimulated invasion and angiogenesis in tumors from Sk_Lu_1 cells.

Conclusions. Our investigation shows a different response to NaVP treatment. Our findings demonstrate that the effects of NaVP on CAM parameters and invasion are cancer-type-specific, and that the pathways critical to the development of tumor invasion differ among various cancer types. Dose-dependent differences of NaVP effect on lung cancer cell lines were observed in previous experiments, but new experiments showed that sodium valproate might act differently depending on dose, and sex and might be cell line specific.

Deep learning-based software for automated cell detection and counting in whole-slide histological image analysis

Edelmers Edgars¹, Fišere Inese²

¹*Institute of Anatomy and Anthropology, Rīga Stradiņš University, Latvia*

²*Surgery Clinic, Pauls Stradiņš Clinical University Hospital, Latvia*

Objectives. This study presents the development of a novel deep learning-based software designed to automate and accelerate routine cell counting in whole-slide histological images. The tool incorporates automatic cell labelling and embedded statistical analysis, aiming to improve both utility and accuracy for clinical and research applications.

Materials and methods. The dataset consists of whole-slide images of large intestine specimens stained for CD117-positive interstitial cells of Cajal, using diaminobenzidine. A deep learning model based on the “You Only Look Once” architecture was trained on 40 annotated images, containing a total of 1,918 manually labelled cells. The model was trained for 100 epochs, using data augmentation, colour deconvolution, and a sliding window technique to manage memory constraints when processing high-resolution images. The Python-based software is capable of processing images with dimensions up to 65,535 by 65,535 pixels on a standard laptop graphics processing unit (Nvidia 3080).

Results. The model achieved a mean average precision of 86 percent at 50 percent intersection over union, with a precision of 85 percent and recall of 80 percent. It processed large whole-slide images within 4 minutes, accurately counting up to 8,857 interstitial cells of Cajal in a single image. The software includes features such as real-time visualization, exportable results, and integrated statistical tools for data analysis. Both the software and the dataset used in this study will be published, making them accessible for future research and development. The results are scheduled for publication in BioMedicine under The Lancet Discovery Science group.

Conclusions. This deep learning solution significantly improves the efficiency, accuracy, and scalability of routine cell counting. By automating the analysis of entire image datasets, it reduces human error and enhances data processing speed, offering valuable utility in both clinical diagnostics and research workflows.

Changes in the vitreous body in residents of radiation-contaminated areas in the early period after a radiation disaster

Fedirko Pavlo¹, Pilmane Māra², Babenko Tetiana¹, Garkava Natalia¹, Dorichevska Raisa¹

¹*Institute of Radiation Hygiene and Epidemiology of National Research Center for Radiation Medicine of National Academy of Medical Sciences of Ukraine, Ukraine*

²*Institute of Anatomy and Anthropology, Rīga Stradiņš University, Latvia*

Objectives. Changes in the vitreous body are one of the least studied radiation-associated effects. These are morphological changes in the vitreous body that cause a change in its transparency. The appearance of changes in the vitreous body was one of the first effects observed after radiation exposure in small doses in residents of radiation-contaminated areas. However, research on this pathology was practically not carried out.

Materials and methods. We reanalyzed the archival results of our examination of the state of the vitreous body in 217 residents of radiation-contaminated areas of the northern regions of Ukraine, conducted in 1992, 6 years after the Chernobyl disaster. Since the standardized method of ophthalmological examination of radiation-exposed persons developed by us was used for examinations during this period, the results can be compared with the data of studies conducted later. Standard modern methods of statistical analysis were used during the reanalysis.

Results. It was established that changes in the vitreous body in the form of cloudiness and significant destruction of the structure were observed in 64 of 217 examined persons (29.5%). The frequency of detection of pathological changes in the vitreous body was statistically significantly higher in the group with a total content of radioactive cesium isotopes of more than 3,700 Bq / whole body, relative risk was 1.968 (1.03–3.75). Morphological changes of the vitreous body were localized mainly in the zone behind the lens and in the central zone. Functional complaints of patients about the presence of cloudiness, flickering, etc. were completely related to morphological changes in the vitreous body.

Conclusions. Thus, already in the period up to 6 years after the radiation incident, a significant increase in the frequency of destruction and clouding of the vitreous body can be observed in the inhabitants of the territories exposed to radiation pollution.

Craniofacial metrics of children aged 1–15 years in Latvia

Grabčika Arta¹, Kažoka Dzintra², Vētra Jānis¹

¹Department of Anthropology, Institute of Anatomy and Anthropology,
Rīga Stradiņš University, Latvia

²Department of Morphology, Institute of Anatomy and Anthropology,
Rīga Stradiņš University, Latvia

Objectives. This study aimed to evaluate the anthropometric characteristics and identify the predominant patterns in craniofacial measurements and indices among children in Latvia.

Materials and methods. The study involved 375 healthy children aged 1 to 15 years in Latvia. The anthropometrical measurements (head circumference, length, width, facial length, and width) were conducted according to the guidelines by R. Martin, K. Saller, and J. Prīmanis at the Anthropology laboratory at the Institute of Anatomy and Anthropology, Rīga Stradiņš University. The instruments (Sieber Hegner & Co., Inc.) included a standard spreading caliper, round-ended caliper, nonstretchable measurement tape, and Vernier caliper. The data were analyzed using descriptive and inferential statistics, by using Microsoft Office Excel and IBM SPSS Statistics 28.0 (IBM SPSS, Armonk, NY, USA). Additionally, the study utilized specific formulas to compute the cephalic index (CI) and facial index (FI).

Results. There were similar patterns of increasing head circumference with age for boys and girls, whereas head length and breadth increased between 1 and 2 years. The mean CI was 77.26 for boys and 77.33 for girls, with an overall mean CI value of 77.30 for children aged 1 to 15. Dolichocephaly was more prevalent in younger ages and decreased over time, while brachycephaly and hyperbrachycephaly remained relatively stable or declined slightly. Mesocephaly exhibited less variation and remained relatively stable across ages. The average FI was 80.51 for boys and 81.06 for girls, with a hyperleptoprosopic face being the most common in the studied population. Significant differences in CI and FI were observed between age groups and sexes.

Conclusions. The craniofacial measurements, including the dimensions of the skull, face and various calculated indices, showed notable variations across the 1-15 age group of Latvian children. These findings are of significant importance, as they have extensive implications, encompassing their relevance in physical anthropology, pediatric fields, medical research and clinical practices.

CAM-Delam – an in vivo assay to visualize and quantify the delamination and invasion capacity of human cancer cells

Green Tami¹, Šlekiene Lina², Gunhaga Lena³

¹ Umea University, Sweden

² Lithuanian University of Health Sciences, Lithuania

³ Department of Medical and Translational Biology, Umea University, Sweden

Objectives. 1. To develop and optimise CAM-Delam assay. 2. To induce metastatic and non-metastatic conditions regarding cancer cells used. 3. To induce ectopic delamination using non-metastatic cell lines followed by recovery using broad spectrum MMP inhibitor.

Materials and methods. Chicken embryos were incubated ex ovo on day 3 using 3 conditions to access the best survival: internal humidified chamber (HC), non-humidified chamber (N-HC) and Petri dish (PD) were used. Cancer cells were then seeded on embryonic day 10 (E10) on chicken embryo chorioallantoic membrane (CAM). 1×10^6 PC-3U-GFP and U251-GFP cells were seeded in the silicon ring on the CAM. After 14h, 1.5 days, 2.5 days and 3.5 days were collected together with CAM. Additionally, non-metastatic U251-GFP were pretreated by hypoxia inducible CoCl_2 followed by broad spectrum MMP inhibitor GM6001. Then immunohistochemistry staining was performed using an anti-Laminin-111 antibody and stained sections were scored for delamination according to 4 categories: intact, altered, damaged and invasion.

Results. Survival of the eggs on day 10 in HC was double compared to N-HC and PD ($p < 0.05$ and $p < 0.01$, respectively). On E13, survival in HC compared to N-HC and PD was significantly higher ($p < 0.001$). PC-3U cells induced minimal alteration of laminin after 14h, followed by the invasion on 3.5 days. U251 cells cultured alone caused minor alterations during the period of 1.5–3.5 days. U251 cells cultured together with CoCl_2 induced laminin damage and cell invasion. Pretreatment with GM6001 (1h) followed by CoCl_2 exposure (24 h) suppressed the effect of the CoCl_2 treatment.

Conclusions. The advantage of the CAM-delam assay is obtaining informative results regarding delamination within a few days to estimate the aggressiveness of human cancer cells and the potential risk for metastasis. It can also be used to study the molecular mechanism, as seen in the study with CoCl_2 and GM6001, that regulate delamination, invasion and formation of micro-metastases.

Histological analysis of chondrosarcoma in an uncommon cranial location: a case report

Jakovļevs Arvīds

Department of Pathology, Rīga Stradiņš University, Latvia

Objectives. To report a rare case of grade 1 chondrosarcoma in the parafalcine region, emphasizing the histological features and the rarity of this anatomical location.

Materials and methods. A 50-year-old patient presented with persistent headaches and seizures. MRI revealed a well-defined mass adjacent to the falx cerebri. Surgical resection of the lesion was performed. The excised tissue underwent routine histopathological examination using hematoxylin and eosin staining. The diagnosis was made based solely on morphological criteria, as the histological features were sufficiently diagnostic.

Results. Gross examination revealed a firm, lobulated mass measuring 3 cm in diameter. Histologically, the tumor exhibited features characteristic of grade 1 chondrosarcoma: minimally increased cellularity, nodular growth pattern, occasional binucleated chondrocytes, mild nuclear atypia. Mitotic figures were rare, and no necrosis was observed. These morphological features confirmed the diagnosis of a low-grade (grade 1) chondrosarcoma. Comprehensive clinical and radiological evaluations found no evidence of other tumors elsewhere in the body, effectively excluding metastatic spread. The parafalcine location is exceptionally rare for chondrosarcomas, which more frequently arise in the skull base. This unusual site suggests a possible origin from embryonic rest cells or metaplastic transformation of meningeal fibroblasts into cartilaginous tissue.

Conclusions. Parafalcine chondrosarcomas are exceedingly rare entities. Awareness of such rare intracranial locations expands the differential diagnosis of parafalcine masses and underscores the importance of considering chondrosarcoma even in atypical sites.

Effects of long-term treatment with a combination of valproic acid and sodium dichloroacetate in rats

Juknevičienė Milda, Balnytė Ingrida, Valančiūtė Angelija, Stakišaitis Donatas

*Department of Histology and Embryology, Faculty of Medicine,
Lithuanian University of Health Sciences, Lithuania*

Objectives. Objectives were to determine the effect of long-term valproic acid and sodium dichloroacetate combination (VPA–NaDCA) treatment on daily diuresis, kidney, blood glucose, and testosterone levels, thymus, and Slc5a8, Slc12a2, and Slc12a5 expression in thymocytes.

Materials and methods. Wistar rats, aged 5–6 weeks, were investigated in VPA–NaDCA-treated gonad-intact both genders and their controls (n = 6 in a group). The 150 mg/kg/day VPA and 100 mg/kg/day DCA combination treatment with drinking water was 4 weeks. Thymocyte Slc12a2, Slc12a5, Slc5a8 RNA expression was determined by real-time PCR; numbers of Hassall's corpuscles (HCs) per 1 mm² of medulla was determined immunohistochemically; height of thick ascending limb (TAL) of Henle loop epitheliocytes was measured in hematoxylin-eosin-stained slides.

Results. VPA–NaDCA increased the rat kidney weight of both genders compared to the corresponding control (p < 0.05). The 28-day treatment increased daily diuresis and K⁺, Na⁺, and Cl⁻ excretion in the male rat's daily urine (p < 0.05). Compared to the control, the excretion of Mg²⁺ in the daily urine of treated females was increased (p < 0.05). Compared to the control, VPA–NaDCA reduced the height of TAL in the female's kidney (p < 0.05). Thymus weight and expression of Slc12a2, Slc12a5 in the female control group were lower than in the male control (p < 0.05); treatment did not affect thymus weight and the expression of Slc5a8, Slc12a2, Slc12a5 in the thymocytes of both genders. The number of HCs was higher in treated males than in the controls (p < 0.05). In comparison with the corresponding control, VPA–NaDCA reduced serum glucose concentrations in rats of both genders and testosterone concentration in males' blood (p < 0.05).

Conclusions. The VPA–NaDCA effect on daily diuresis, monovalent and divalent ions excretion, TAL height in the kidney, and HCs number in the thymus is gender-related. The VPA–NaDCA treatment reduces blood glucose and testosterone levels in the blood.

Human olecranon parameters and shapes variability: insights from “Anatamage” study

Kažoka Dzintra, Pilmane Māra

*Department of Morphology, Institute of Anatomy and Anthropology,
Rīga Stradiņš University, Latvia*

Objectives. This study aimed to measure various parameters and analyze the shapes of the olecranon, identifying their variations in virtual human bodies.

Materials and methods. The study, conducted from July to August 2024, utilized the geometric morphometrics method to analyze digital images of the olecranon from two male and two female cadavers. These images were sourced from the virtual dissection table “Anatamage” of the Department of Morphology. The study revealed shape variabilities in the olecranon across both sides. The same research team took the photographs, capturing a medial view of each olecranon. The images were captured during a single session. A series of five landmarks (LM) and four semilandmarks (SLM) were digitized using geometric morphometric analysis with the open-source software “ImageJ” Firstly, all landmarks were allocated on each image, and then semilandmarks were added. Two parameters, maximum width and maximum length of olecranon, were also measured. Grouping procedures were performed on the olecranon across bodies, examining the differences in parameters and shape. Morphological variations were analyzed using Microsoft Excel and IBM SPSS Statistics 26.0 descriptive statistics.

Results. Eight images with 40 LM and 32 SLM were obtained to reveal the morphological differentiation among virtual bodies. The olecranon, the bony prominence of the elbow, had several distinct shapes and showed variability between males and females. Males tend to have more extensive and more robust olecranons compared to females. The olecranon on the dominant arm was more developed and showed differences in shape and size. The top of the olecranon curved differently anteriorly, forming a prominent tip for the olecranon fossa of the humerus. The shape of the articular surface of the olecranon for humerus interaction varied noticeably.

Conclusions. The olecranon, part of the forearm bone, showed different parameters and shapes. Current data and anatomical knowledge about this structure variability benefit anatomists, anthropologists, orthopedic surgeons, and radiologists.

Variability in ear morphology among virtual human bodies: insights from digital measurements

Kažoka Dzintra, Pilmane Māra

Institute of Anatomy and Anthropology, Rīga Stradiņš University, Latvia

Objectives. The study aimed to measure various anthropometric dimensions and features of the virtual adult human ear to understand its symmetry, size and shape.

Materials and methods. On the virtual dissection table “Anatomage” images, various landmarks of the auricle were located and identified. Several parallel and perpendicular lines were created and extended to the borders of the auricle to guarantee thorough data gathering for each auricle of four virtual human bodies on bilateral sides. After placing, fixing, and positioning the ear on the touch screen, nine measurements (including concha length and width, lobule height and width, tragus length, ear length above and below the tragus, ear length and width) were taken. The main investigator made all measurements with a digital roller. The information was organized into a table for every virtual human body. Two groups were formed according to the sexes (2 males and two females) and ethnicity (Caucasian and Asian). The data were obtained for statistical analysis using Excel and compared between the groups.

Results. The study obtained unique and intriguing insights into the ear morphology of observed virtual human bodies. Each image exhibited distinct ear features, such as unique curves and contours. An important finding was the variability observed in the presence of attached or free lobules among the virtual human bodies. The external ears demonstrated marked asymmetry, with dimensions and characteristics differing across genders and ethnicities. Furthermore, variations in the size and position of the intertragic notch were also detected between sides and obtained groups. Additionally, diverse external ear shapes were identified, adding to the intrigue of the study’s findings.

Conclusions. The digital measurements adopted in the study for detection of ear dimensions showed potential role in ear morphometry. It is essential to know the typical and normal dimensions of the ear to identify any acquired ear abnormalities, congenital malformations or syndromes.

Exploring the diverse branching patterns of Arbor Vitae

Kuļibaba Georgijs¹, Kažoka Dzintra²

¹Faculty of Medicine, Rīga Stradiņš University, Latvia

²Institute of Anatomy and Anthropology, Rīga Stradiņš University, Latvia

Objectives. The study aimed to characterize the patterns of the Arbor Vitae and identify any branching variations.

Materials and methods. Fourteen specimens of Arbor Vitae were meticulously analyzed and measured using materials provided by the Department of Morphology at the Institute of Anatomy and Anthropology. Precise measurements of each branch's length and the overall branching count of the Arbor Vitae were obtained using a digital caliper and tools from the open-source image processing program "ImageJ". The collected data, which revealed a diverse range of branching variations, were subjected to comprehensive statistical analysis using Microsoft Excel.

Results. Upon conducting a comprehensive analysis, it was determined that the structural characteristics of Arbor Vitae branches exhibit variability, and specific, discernible patterns can be distinguished. Three potential variations of Uvual branch divisions have been observed, with the branch typically splitting into three or four smaller branches. In some cases, the Uvual branch displayed a double bifurcation. Additionally, two variations of the Culmen Tree division have been identified, showing a tendency to divide into two or three smaller branches. The findings suggest a potential correlation between the number of Culmen Tree divisions and its length before splitting at the end. Furthermore, the data indicated that the Pyramis branch tends to be the longest, while the Uvual branch tends to be the shortest. The Lingula branch had the fewest divisions, comparing the Pyramis branch, with the most divisions.

Conclusions. Each Arbor Vitae exhibits unique characteristics with clearly defined and distinct patterns. The bifurcation of Culmen Tree and Uvual branches provides insight into these patterns. Typically, the Uvual branch and Culmen Tree bifurcate into three branches at their terminal parts. These observations imply a potential connection between the number of Culmen Tree bifurcations and the length of its branches in the anatomical structure of the Arbor Vitae.

Morphological changes of angiotensin II type 2 receptor at myenteric plexuses of diverticular disease in the human gastrointestinal tract

Lapeikis Ignas¹, Rysevaite-Kyguoliene Kristina¹,
Malinauskas Mantas², Paužienė Neringa¹

¹*Institute of Anatomy, Faculty of Medicine, Lithuanian University of Health Sciences, Lithuania*

²*Institute of Physiology and Pharmacology, Faculty of Medicine, Lithuanian University of Health Sciences, Lithuania*

Objectives. Angiotensin II peptide involved in regulating blood pressure and electrolyte balance. An increase of angiotensin II receptor type 2 (AT2R) at myenteric plexus (MP) in the gastrointestinal tract could lead to heightened activity in this area. Increased expression of AT2R and neuronal bodies may have an effect on peristalsis in the gastrointestinal tract¹. The aim of this study is to determine neurons positive for AT2R and neuronal bodies count in MP of diverticulosis patients

Materials and methods. Specimens for the symptomatic diverticular disease (SDD) group were obtained from patients who underwent sigmoid resection for diverticulitis; control from patients undergoing surgery for non-obstructing colorectal carcinoma without symptoms of complicated or uncomplicated diverticular disease. Preparations were stained immunohistochemically with antibodies against HuC/HuD (general neuronal marker) and antibodies against AT2R. The general number of neurons (positive for HuC/HuD) and neurons positive for AT2 receptors was counted, and area of 50 myenteric ganglions in each group was measured using the ImageJ program. The data expressed as a number of neurons/10000 μm^2 . The statistical data were calculated using SPSS 29.0 (using one-way ANOVA test).

Results. The average area of myenteric ganglion was 15000 μm^2 in both groups and varied from 2056 μm^2 to 66884 μm^2 in the control group and from 2338 μm^2 to 40162 μm^2 in the SDD group. The number of HuC/HuD positive neurons per 10000 μm^2 was 9/10000 μm^2 in SDD and 7/10000 μm^2 in control and showed statistical significance ($p = 0.046$). A number of AT2R positive neurons was statistically significantly ($p = 0.023$) higher in SDD 4/10000 μm^2 comparing with control (3/10000 μm^2).

Conclusions. The elevated AT2 receptor expression and neuronal bodies count in SDD suggests a possible effect on peristalsis of gastrointestinal tract on diverticulosis patients comparing them with colorectal cancer patients.

¹ Zizzo, M. G., Auteri, M., Amato, A., et al. Angiotensin II type II receptors and colonic dysmotility in 2,4-dinitrofluorobenzenesulfonic acid-induced colitis in rats. *Neurogastroenterol Motil.* 2017; 29(6). doi:10.1111/nmo.13019

Morphometrical parameters of 31–35-year-old men testes

Lasiene Kristina¹, Radzeviciute Simona², Gasiliunas Donatas²,
Juodziukyniene Nomeda², Zilaitiene Birute², Dabužinskiene Anita²

¹*Department of Histology and Embryology, Academy of Medicine,*

Lithuanian University of Health Sciences, Lithuania

²*Lithuanian University of Health Sciences, Lithuania*

Objectives. To measure and compare some morphometrical parameters of the left and right testes in 31–35-year-old men.

Materials and methods. This work was approved by Kaunas Region Biomedical Research Ethics Committee (No. P2-BE-2-1/2015, 2022-05-06). Pairs of testes from 5 men aged 31–35 years were obtained from Kaunas Division of State Forensic Medicine Service after autopsy.

The standard hematoxylin-eosin staining protocol of histological slides was used. The thickness of the Tunica albuginea (30 measurement/testis), the diameter of seminiferous tubules and the thickness of seminiferous epithelium (20 tubules/testis), the diameter of spermatogonia nuclei and Leydig cells nuclei (30 cells/testis) were measured using the cellSens Dimension 1.9 Digital Imaging Software package. The IBM SPSS Statistics program independent Samples T-Test was used for statistical comparison of the left and right testes' parameters (p values).

Results. The left testes had significantly thinner ($510.76 \pm 154.66 \mu\text{m}$) Tunica albuginea than the right ones ($570.82 \pm 175.94 \mu\text{m}$; $p < 0.05$).

The diameter of seminiferous tubules in the left testes was slightly larger than the right ones ($206.72 \pm 37.42 \mu\text{m}$ and $204.74 \pm 34.75 \mu\text{m}$ respectively; $p > 0.5$).

The seminiferous epithelium of the left testes' seminiferous tubules ($59.5 \pm 15.33 \mu\text{m}$) was thicker than in the right ones ($58.6 \pm 15.19 \mu\text{m}$; $p > 0.05$).

The diameter of spermatogonia nuclei in the left testes' seminiferous tubules was significantly major than in the right testes ($5.87 \pm 0.92 \mu\text{m}$ and $5.64 \pm 1.07 \mu\text{m}$ respectively, $p < 0.05$).

The diameter of Leydig cells nuclei of the left testes ($6.28 \pm 1.2 \mu\text{m}$) was insignificantly major than of the right ones ($6.23 \pm 1.21 \mu\text{m}$, $p > 0.05$).

Conclusions. In the left testes, the Tunica albuginea was significantly thinner, and the diameter of seminiferous tubules, the thickness of seminiferous epithelium, the diameter of spermatogonia and Leydig cells nuclei were larger than in the right testes.

Results of arterial blood pressure in pre-school aged children in Riga region

Martinsone-Bērzkalne Liene¹, Umbraško Silvija¹, Asare Lāsma²

¹*Institute of Anatomy and Anthropology, Rīga Stradiņš University, Latvia*

²*Statistics Unit, Rīga Stradiņš University, Latvia*

Objectives. The World Health Organization presents the data about hypertension in 2021: 1.28 billion adults aged 30–79 years had arterial hypertension. American Heart Association (AHA) offers the definition of ideal cardiovascular health for children that consists of seven metrics: health behaviours (having a healthy weight status, being sufficiently physically active and eating cardiovascular – healthy diet) and health factors (healthy levels of total cholesterol, blood pressure and glucose). The aim of our research was to clarify the data of arterial blood pressure in children aged 3–7 years in Riga region for the first time in anthropology research.

Materials and methods. The research included 1083 children aged 3–7 years: 515 boys and 568 girls from 28 Riga region preschool education institutions in the time period 2019–2022. Anthropometric measurements were performed by methods of K. Saller and R. Martin (1957). The blood pressure was measured with portable electric device “Omron”. Three measurements were taken for each child, the average measurement was recorded.

Results. The mean systolic blood pressure for 3 years old boys was 101.12 ± 13.6 mmHg, in the group of 4 years old boys 93.8 ± 12.6 mmHg, in the group of 5 years old boys 96.3 ± 13.7 mmHg, in the group of 6 years old boys 96.7 ± 11.9 mmHg, in the group of 7 years old boys 102.1 ± 12.1 mmHg. The data about mean diastolic pressure for boys, arterial pressure for girls, minimal and maximal indicators and correlations with related indicators were obtained.

Conclusions. The obtained data showed a strong correlation between arterial blood pressure and body weight and height, body mass index, annual increase in weight and height, also physical activity behaviours.

Spatially and temporally restricted expression of BMP-2 and Shh during early development of human embryo spinal cord

Namm Aimar, Arend Andres, Torga Taavi, Aunapuu Marina

Institute of Biomedicine and Translational Medicine, University of Tartu, Estonia

Objectives. Early embryological studies mainly have been made on experimental animals identified two of the best-known morphogenetic proteins. Sonic hedgehog (Shh) signalling is produced by the floor plate of the forming spinal cord induces ventral cell types in a concentration dependent manner, while Bone morphogenetic proteins (BMP-s) are produced by roof plate to promote dorsal identities. Both BMP-s and Shh either induce or repress the expression of homeodomain proteins, creating a unique expression pattern of transcription factors in each progenitor domain of the developing spinal cord. Only limited results exist about the developmental role of these proteins in the human spinal cord development.

Materials and methods. The expression of BMP-2 and Shh was examined in 23 human embryos by immunohistochemistry. The embryos were collected after legal abortions, fixed in 4% paraformaldehyde, embedded in paraffin and tissue blocks were serially cut in transversal direction. The embryos were classified according to Carnegie stages. For immunohistochemistry the slices were incubated with primary antibodies and with a universal secondary antibody.

Results. Our data demonstrate spatial and temporal expression of BMP-2 and Shh in the spinal cord of CS 14 to 20 in human embryos. We detected higher expression of BMP-2 in the dorsal part and remarkable expression of Shh in the ventral part of the developing spinal cord. However, variations seem to exist in immunostaining intensity at different developmental stages. In the case of both studied proteins, there was a tendency for the expressions to decline in the later stages of development.

Conclusions. Across the vertebrate subphylum the dorsal-ventral patterning of the developing spinal cord remains largely similar, the same set of signals simultaneously controls tissue growth and neural patterning. Our findings support the theory about the important role of BMP-2 and Shh in the regulation of the cellular proliferation and patterning of the developing spinal cord in the human embryos.

Expression of NaV1.2 in the hippocampus and cerebellum of epilepsy patients

Naumovs Vladimirs¹, Skuja Sandra², Groma Valērija²

¹ "Gintermuiža" Hospital, Latvia

² Institute of Anatomy and Anthropology, Rīga Stradiņš University, Latvia

Objectives. Neuronal voltage-gated sodium channels (VGSCs) have been implicated in the development of ictal events in human epilepsy. Five known isoforms of the VGSC family are expressed in the central nervous system (CNS). NaV1.2 has been reported to be dominantly expressed in the excitatory neurons of the CNS. The expression of VGSC isoforms varies throughout the CNS both spatially and temporally, as well as within individual neurons. This differential expression reflects functional variability across the VGSC family. However, data on the expression of VGSC isoforms in the CNS of human epilepsy patients is limited.

Materials and methods. Autopsy material from four epilepsy patients has been acquired from the Netherlands Brain Bank. The hippocampus and cerebellum have been selected for analysis. Immunohistochemical staining for NaV1.2 has been performed, and a semi-quantitative assessment has been conducted.

Results. NaV1.2 immunoreactivity (IR) has been observed in both the cerebellar and hippocampal regions of all epilepsy patients. Grey matter showed more prominent staining than white matter in both areas. Prominent NaV1.2 IR has been noted in the pyramidal cell layer throughout the hippocampal formation (CA1 to CA4), while no IR has been observed in the polymorphic and molecular layers or white matter. Interestingly, NaV1.2 IR has been predominantly observed in the nuclei of pyramidal cells. Of the pyramidal cell nuclei, 31.50% (range: 17.33–49.33%, n = 60) have shown NaV1.2 IR. In the cerebellum, both granular cell nuclei and the neuropil of the granular cell layer have shown marked NaV1.2 IR, while Purkinje cells and the molecular cell layer showed no notable NaV1.2 IR. In the granular cell layer, 30.33% (range: 17.33–58.67%, n = 60) of cell nuclei showed NaV1.2 IR.

Conclusions. The difference in NaV1.2 IR between hippocampal pyramidal cells and cerebellar granular cells is not statistically significant, suggesting that both regions could be similarly affected in epilepsy.

A pilot study of cells in human plantar fascia exposed to chronic ischemia due to atherosclerosis

Palubinskienė Jolita¹, Gorodetsky Michael Lior², Kilimaitė Evelina¹, Lekšas Mindaugas³

¹*Department of Histology and Embryology, Faculty of Medicine,
Lithuanian University of Health Sciences, Lithuania*

²*Faculty of Medicine, Lithuanian University of Health Sciences, Lithuania*

³*Lithuanian University of Health Sciences, Lithuania*

Objectives. The human plantar fascia (PF) is a tendon-like structure that some regard as a plantar aponeurosis. It provides attachment to muscles and supports the arch of the plantar side of the foot. In earlier studies on the histological structure of PF, chondrocytes were found within its dense connective tissue (CT), suggesting that the CT cells change in response to chronic conditions like diabetes mellitus (DM). This study aims to explore whether chronic ischemia of the CT, as seen in peripheral artery disease (PAD), results in chondrocyte differentiation from fibrocytes.

Materials and methods. Forty-six paraffin-embedded blocks (2.0 x 0.5 cm) of the central part of the PF were obtained from amputated feet with PAD (N = 16), DM (N = 4), and acute conditions (AC, N = 3). Each sample was sectioned along the collagen fibers at a thickness of 3 μm and stained with H&E. Two visual fields per slide were examined using x10 objective lens of an OLYMPUS BX40F4 microscope, and images were captured with a digital camera. Measurements of the total count of cells and chondrocytes (if present) were taken, and the number of cells per mm^2 was calculated. Chondrocytes were identified by their round or oval nucleus, pale-stained cytoplasm, and basophilic territorial matrix.

Results. The average area per investigated field was $315,235.8 \mu\text{m}^2$. The average number of cells per mm^2 was 261.3 in the DM group, 218.7 in the PAD group, and 281.6 in the AC group ($p > 0.05$, Mann-Whitney U and t-test). Chondrocytes accounted for 28.5%, 14.5%, and 6.9% of cells in the DM, PAD, and AC groups, respectively. Significant differences were observed in chondrocyte percentage between the DM and AC groups ($p < 0.05$).

Conclusions. A tendency that chronic ischemia causes chondrocyte differentiation from fibrocytes in PF was observed, statistically significant difference not achieved due to too few cases examined in the control group.

Morphopathogenic factors of neonate intra-abdominal adhesions: a pilot study

Pauliņš Arvis¹, Pilmane Māra²

¹ Rīga Stradiņš University, Latvia

² Institute of Anatomy and Anthropology, Rīga Stradiņš University, Latvia

Objectives. Newborns' intestinal adhesions have been reported in 4.7% of infants who underwent a laparotomy, but they can also appear idiopathically. The etiology and pathogenesis of adhesions are still to be determined, but evidence shows a connection with inflammation, formation of fibrin bands, hypoxia and tissue remodeling. Multiple candidate genes have been associated with adhesion development. This study evaluates the appearance of Sonic Hedgehog (SHH), Indian Hedgehog (IHH), Forkhead-box-F1 (FOXF1), caudal-type homeobox-1 (CDX1), HCLS1-associated protein-X-1 (HAX-1), GATA-Binding-Protein-4 (GATA4) and Granzyme-B (GZMB) proteins in neonatal adhesions and describes possible interfactorial correlations.

Materials and methods. Adhesion-affected samples were collected from 14 patients under one year of age that underwent abdominal surgery to treat intestinal obstruction. The control group consisted of 6 individuals that had surgical repairment of inguinal hernia. Routine staining and immunohistochemistry were performed. Immunopositive fibroblasts, macrophages, endotheliocytes, smooth muscle myocytes of blood vessels and mesotheliocytes were investigated and evaluated semi-quantitatively. Statistical analysis was done using non-parametric tests, and correlations were calculated based on Spearman's correlation analysis.

Results. A statistically significant decrease was observed for SHH, IHH, FOXF1, GATA-4 and partially for GZMB gene proteins in the patient group. A similar expression of all the factors in both patients' and control's mesothelium was detected. A strong positive correlation was seen between the number of FOXF1 and GATA4 positive endotheliocytes; between FOXF1 and GZMB/CDX1 positive cells in blood vessels; between SHH/IHH/GATA4/GZMB/CDX1 positive fibroblasts and macrophages; between GATA4 positive fibroblasts and HAX-1 macrophages; between GATA4 and CDX1 positive endotheliocytes; between the number of GZMB and CDX1 positive endotheliocytes.

Conclusions. SHH, IHH, FOXF1, GATA-4 and GZMB gene proteins might have a role in neonatal adhesion development which could suggest a dysregulation of cellular events. Abundance of correlations between the gene protein appearances in different structures indicate the affected blood vessels, fibroblasts and macrophages, however, mesothelium seems not to be involved in the morphopathogenesis.

Comparison of healthy and diseased free-stall barn cow milk microbiota, cytokines and antimicrobial proteins in seasonal aspect

Pilmane Māra¹, Lohova Elizabeta¹, Melderis Ivars¹, Gontar Lukasz², Kochanski Maksymilian², Drutowska Andzelika², Prieto-Simon Beatriz³

¹Institute of Anatomy and Anthropology, Rīga Stradiņš University, Latvia

²Pro-Akademia, Poland

³Universitat Rovira i Virgili, Spain

Objectives. Bovine mastitis is still challenging in the dairy industry. The invasion of udder by pathogens induces mastitis. Despite the experimentally induced mastitis the research on free-stall barn mastitis is limited and practically absent is the seasonal character of the mastitis inducers.

Materials and methods. Milk from 15 Holstein Friesian cows was used. Cows were divided into 3 groups: 5 healthy, 5 subclinical and 5 clinical animals. Samples were tested using immunohistochemistry for IL-2,-4,-10,-17A, TGF- β 1 and β -Def 3. The milk microbiota in the spring and autumn seasons was detected. Statistics were performed to compare protein expression over time and status.

Results. High expression of IL-2, IL-4, IL17A, TGF- β 1 was detected in healthy, subclinical and clinical mastitis cows. Expression of IL-10 and β -Def 3 in the milk of healthy cows was high with a significant decrease in infected cows. *S.uberis* and *S.aureus* prevailed in the milk without seasonal preference. Seasonal were rarely detected *E. coli* and *S. agalactiae*, while *Klebsiella*, *Enterobacter*, *Citrobacter spp.* were seen mainly in the spring milk. All the detected cytokines varied in spring but returned to high expression in the autumn. In milk from cattle with clinical mastitis, the most cells were IL-2-positive, followed by IL-17A cells, but IL-4 and TGF- β 1 increased more in autumn.

Conclusions. The stable expression of IL-2,-4,-17A and TGF β -1 from day 4 to day 14 in the milk of subclinical and clinical mastitis affected and in the healthy cows' milk indicates the possible insignificant role of these cytokines in mastitis. Decreased expression of IL-10 and β -Def 3 in the milk of subclinical and clinical mastitis indicates the significance of these factors for the diagnosis. The number of ILs positive cells in the milk of cows with subclinical mastitis has the greatest variation and decreases in spring, indicating the beginning of summer as an exhaustion of the immune system and autumn as the local immunity restoration time.

Body donation in Latvia during the last 30 years

Pilmane Māra¹, Kažoka Dzintra¹, Vētra Jānis¹, Gardovskis Jānis², Pētersons Aigars³

¹*Institute of Anatomy and Anthropology, Rīga Stradiņš University, Latvia*

²*Department of Surgery, Rīga Stradiņš University, Latvia*

³*Rīga Stradiņš University, Latvia*

Objectives. The description of the changes in body donation in Latvia.

Materials and methods. Legislative sources, mass media, RSU and AAI documents.

Results. The sovereignty of Latvia was restored on 04-05-1990. From 1993, the reception of a dead person in the Anatomicum was determined by the law “On the protection of the body of a dead person and the use of human tissues and organs in medicine”, which provided for the acquisition of a corps if the will of a person was documented during the life; if all first-degree relatives had given their consent and if the unclaimed person’s will was unknown. On 13-06-2019, amendments to the law determined the use of one’s body only after the clarification of the will expressed during the life of a deceased person.

Since the 1990ies, Anatomicum has worked with highly ethical standards and expressed public gratitude to the people who wished to donate themselves. For the first time, the RSU held a commemoration for these people in 2002. At that time, the ashes of dissected people from the Soviet era were cremated. The second Thanksgiving service was held on 04-12-2012 in the Anatomicum, but on July 3, 2015, for the first time, the burial of previously cremated ashes was held publicly in the Mārtiņš Cemetery. This was attended by priests of the Latvian Evangelical Lutheran and the Latvian Orthodox Churches, the Catholic Church and the Union of Baptist Churches. The second such funeral took place on 28-09-2022. A monument was erected in the yard of Anatomicum to those who donated themselves and/or were dissected. On average, 2–3 articles on the topic of self-donation are published in mass media per year.

Conclusions. Thanks to publicly organized events of a highly ethical nature and regular explanations in the mass media, Latvian society has strengthened its belief in the necessity of donating.

Distribution of genes and their proteins in Ladd's band tissue

Pivrika Evelīna¹, Pētersons Aigars¹, Junga Anna², Pilmane Māra²

¹Rīga Stradiņš University, Latvia

²Institute of Anatomy and Anthropology, Rīga Stradiņš University, Latvia

Objectives. Ladd's bands belong to congenital intra-abdominal adhesions – they are fibrous ligaments that extend from the colon to the abdominal wall. The main cause is associated with abnormal intestinal rotation during the embryonic period, and these links can lead to small bowel obstruction. The expression of certain genes – CDX1, SHH, IHH might be associated with intestinal malrotation and contribute to the formation of Ladd's ligaments; thus, we aimed to detect these genes and their proteins.

Materials and methods. Specimens of 10 patients with Ladd's band obtained during the first adhesion removal surgery were analyzed. The material of 8 patients obtained during inguinal hernia surgery developed the controls. Gene (CDX1, IHH, SHH) expression was analyzed by in situ hybridization and their proteins – by immunohistochemistry. Positive cells were counted semi-quantitatively. The Spearman correlation coefficient was used to clarify the relationships between the factors.

Results. CDX1 protein appeared in an increased number of fibroblasts, in some macrophages, and decreased in endotheliocytes, mesotheliocytes of patients. The same gene appeared just in some fibroblasts. SHH protein showed an increased number of fibroblasts, endotheliocytes, mesotheliocytes and macrophages in patients, while the same gene was detected in an indistinct number of fibroblasts of adhesions. Finally, a similar number of IHH protein positive different cell types was detected in both – patients and controls. Some moderate correlations were observed between different cells of SHH and selectively between CDX1 endotheliocytes only.

Conclusions. SHH protein dominance in Ladd's bands moves this protein as significant in this adhesion type pathogenesis. An increase of fibroblasts and their rich expression for gene proteins underlines this type of cell for the development of embryonic adhesions. IHH seems not to be involved in the Ladd's bands formation. SHH and CDX1 gene proteins, but not the same genes, are players in the Ladd's bands formation.

Effect of multi-stressor training on the antioxidative system

Pļaviņa Liāna

Institute of Anatomy and Anthropology, Rīga Stradiņš University, Latvia

Objectives. High physical and psycho-emotional load, fatigue, and sleep deprivation during the multi-stressor environment contribute to the increased formation of reactive oxygen species (ROS) and cell damage. Physical activity can have various effects on the body, including changes in antioxidative capacity. Our study aimed to investigate the effect of a 10-day-long multi-stressor training on the antioxidative system damage.

Materials and methods. The study group included 75 healthy persons aged from 23 to 34 years. They participated in ten days long (total 24 hours) high intensity physical training with aerobic and strength training elements in combination with related energy deficiency. The antioxidative system activity was investigated by detection of superoxide dismutase activity (SOD), and total antioxidants capacity (TAC), glutathione system markers in plasma. Participants tested before physical training directly after ten day long of physical training.

Results. Analysis of parameters dynamic before and after high physical load in multi-stressor environment revealed correlated changes of antioxidative system activity. We found the correlation between, oxidative stress parameters and physical fitness level by using Spearman's correlation analysis. Effects of the training included an increase in GSSH and GSH and a decrease in H₂O₂, SOD, 8-OHdG, and MDA levels. Simultaneously, the OS index also decreased after the training course.

Conclusions. Analysis of parameters dynamic before and after high physical load in multi stressor environment revealed corelated changes of antioxidative system activity. We found the correlation between oxidative stress parameters and physical fitness level by using Spearman`s correlation analysis. Effects of the training included an increase in GSSH and GSH and a decrease in H₂O₂, SOD, 8-OHdG, and MDA levels. Simultaneously, the OS index also decreased after the training course.

Changes in neuropeptides expression in the jugular and nodose ganglion of the vagus nerve in arterial hypertension during the age

Rysevaite-Kyguoliene Kristina, Novikova Jekaterina, Paužienė Neringa

Institute of Anatomy, Faculty of Medicine, Lithuanian University of Health Sciences, Lithuania

Objectives. The study aims to determine the effects of arterial hypertension on the structure and neuropeptides expression of the vagus nerve sensory ganglia in young and old rats.

Materials and methods. SHR (spontaneously hypertensive rats) and WKY (Wistar Kyoto rats) of different ages (8, 40 and 60 weeks) were used in the study. In each group, sections of the left and right nodose and jugular ganglia of three rats were examined immunohistochemically using antibodies against PGP9.5, CGRP, nNOS, and TTN3.

Results. With aging, in the SHR group, the diameter of neurons in both ganglia decreases. Meanwhile, in control rats, at 60 weeks of age, only the neurons of the nodose ganglion are decreasing. In arterial hypertension, the expression of CGRP and nNOS is increased in the jugular ganglion. Meanwhile, CGRP expression in the nodose ganglion increased with age in both SHR and WKY groups, but nNOS expression in the nodose ganglion at 60 weeks of age in the SHR group, the reduction is about 50 percent. TTN3 expression in the jugular ganglion decreases with age in the SHR group. Meanwhile, in the nodose ganglion, TTN3 expression increases with age.

Conclusions. The results of this study demonstrate different expressions of investigated neuro-markers in two different vagus nerve ganglia. The revealed significant quantitative differences in neuro-markers expression during the age in both groups, SHR and WKY, suggests, that not only hypertensive disease influence the expression of neuropeptides, but also there is natural changes of neuropeptides expression in old age of animals.

Galectin-10 characterization in cleft lip palate (CLP) – affected palatal tissue

Rone Alise Elizabete, Pilmane Māra

Institute of Anatomy and Anthropology, Rīga Stradiņš University, Latvia

Objectives. Cleft lip palate is one of the most common craniofacial birth defects, caused by multiple defence factors involved in failure in palatal shelf elevation, fusion, and, most importantly, chronic inflammation. Gal-10 involvement in different local inflammatory processes has been discussed before, however knowledge of local tissue inflammation in postnatal cleft palate and tissue regeneration is scant. This study focuses on detection and possible role of Gal-10 in cleft affected tissue in the ontogenetical aspect.

Materials and methods. Craniofacial cleft tissue material was obtained from 21 children aged varying from 8 months to 12.7 years with milk or mixed dentition undergoing surgery for non-syndromic craniofacial cleft diagnosis. Control groups for milk dentition were 5 subjects without orofacial defects and 3 subjects with lip frenula surgery for mixed dentition. The number of factor positive cells in control and patient group tissue was evaluated by using the semiquantitative counting method, later evaluated by nonparametric statistical methods.

Results. Gal-10 was found in elevated levels in epithelium in correlation with age, from milk to mixed dentition, as well as in both the control and patient samples. Notable differences in expression can be seen when comparing milk and mixed dentition patient muscle tissue, where the milk dentition palate shows more elevated levels of Gal-10 in comparison to the mixed dentition palate.

Conclusions. Almost the absence of Gal-10 in healthy palate with an increase of expression in palatal epithelium from milk to mixed dentition age of cleft-affected children suggests its possible role to provide local defence and epithelium barrier function. Palatal muscles are not the main place for Gal-10 expression neither in healthy nor cleft affected individuals. The sporadic and insignificant appearance of Gal-10 in healthy milk dentition and mixed dentition group of cleft-affected palatal connective tissue prove the individual changes in the palatal tissue, which do not depend on the specific disease.

Abundance, morphology and innervation of cardiac small intensely fluorescent cells

Sabeckis Ignas, Rysevaite-Kyguoliene Kristina, Pauža Dainius Haroldas

Institute of Anatomy, Faculty of Medicine, Lithuanian University of Health Sciences, Lithuania

Objectives. This study was aimed to investigate the small intensely fluorescent (SIF) cells: their morphologic pattern, distribution, abundance and relationship with afferent vagal nerve fibers positive for neuronal nitric oxide synthase (nNOS).

Materials and methods. We have analyzed 5463 SIF cells found in n = 3 mature Wistar rats of both genders. Flat whole-mount atrial preparations were made employing immunohistochemical staining for tyrosine hydroxylase (TH), neuronal nitric oxide synthase (nNOS) and choline acetyltransferase (ChAT). Imaging of SIF cells and neuronal structures was performed using a confocal laser scanning microscope, while their calculations – the FIJI 2.15.1 software.

Results. The revealed TH (+) SIF cells were distributed within 685 clusters that involved from several to 111 SIF cells per cluster. The clusters enclosed two morphotypes of SIF cells. Type I cells had elongated SIF cell bodies with 1–3 processes, while Type II – SIF cells were lacking processes. 37.5% of the clusters involved Type I cells, 19.6% – Type II, yet 42.6% – exhibited SIF cells of both phenotypes. 47.7% of SIF cell clusters were localized on a nerve, 17.2% – adjacent to a nerve, 9.8% – in a ganglion, 19.1% – nearby ganglia and 6.1% were isolated from any neuronal structure. We identified three patterns of SIF cells interactions with nNOS(+) nerve fibers: (1) 2.3% of SIF cells had adjacent axons with numerous varicosities, (2) 19.6% – only a few nearby axons with varicosities, and (3) 77.8% were free of any neighbouring nerve fibers.

Conclusions. Cardiac SIF cells in rats are of two phenotypes. Their clusters mostly distribute on nerves or nearby ganglia, but only 2.3% of SIF cells have evident neural links with nNOS(+) axons. These findings suggest the special role of the limited number of SIF cells innervated by vagal afferents in cardiac neural regulation.

Effects of environmentally relevant concentrations of phthalates on first generation rat embryo body and bone length

Sėrikovaitė Evita¹, Alčauskaitė Justina¹, Paulikaitė Edita², Skujienė Grita²,
Žalgevičienė Violeta², Aukštikalnienė Rasa³

¹Faculty of Medicine, Vilnius University, Lithuania

²Institute of Biosciences, Life Sciences Centre, Vilnius University, Lithuania

³Department of Anatomy, Histology and Anthropology, Institute of Biomedical Sciences,
Faculty of Medicine, Vilnius University, Lithuania

Objectives. Phthalates, widely used plasticizers, are found in wastewater and subsequently in the human body, linking them to impaired bone formation in embryos. This study aims to identify their effects on body and bone length in female rat embryos.

Materials and methods. 36 F0 female Wistar rats were divided into 6 groups, based on phthalate dosage: control (K), received a phthalate-free diet; DEHP_200 – 200 µg/kg di(2-ethylhexyl) phthalate (DEHP); DEHP_1000 – 1000 µg/kg DEHP; DBP_100 – 100 µg/kg dibutyl phthalate (DBP); DBP_500 – 500 µg/kg DBP; DEHP_DBP – 200 µg/kg DEHP and DBP_100 µg/kg DBP. The rats received diets daily for two months, were mated, and euthanized on the 21st day of embryogenesis. Embryos were fixed according to the whole-mount skeletal staining protocol. Embryo lengths and the lengths of the humerus, ulna, radius, femur, tibia, and fibula were measured using a stereomicroscope and NIS-Elements D software.

Results. Embryo lengths in the DEHP_1000 were longer than in K, DEHP_200, and DEHP_DBP groups (4.02 > 3.86; 4.02 > 3.76; 4.02 > 3.76). The DBP groups showed no significant results. Regarding bone lengths, ulnar, radial, tibial, and fibular bones were significantly longer in the DEHP_1000 group compared with DEHP_200 (4.35 > 3.81; 3.40 > 3.06; 3.82 > 3.27; 3.74 > 3.31). In the DEHP_200 group, ulnar, radial, and tibial bones were significantly shorter than in the K group (3.81 < 4.21; 3.06 < 3.34; 3.27 < 3.64). All measured bone lengths (humeral, ulnar, radial, femoral, tibial, and fibular) in the DBP_100 group were significantly shorter compared with the K group (3.68 < 4.04; 3.91 < 4.21; 3.10 < 3.34; 2.83 < 3.13; 3.29 < 3.64; 3.20 < 3.47). In the DEHP_DBP group, femoral bones were significantly shorter than in the K group (2.83 < 3.13), and fibular bones were shorter than in the DEHP_1000 group (3.15 < 3.74).

Conclusions. In conclusion, embryos and measured bones are longer in groups with higher phthalate doses, while they are shorter in groups with lower doses compared to the control group. In addition, the dose-response relationship appears to be non-linear.

A comparative study of effectiveness of sodium dichloroacetate and temozolomide on glioblastoma xenograft growth

Skredenienė Ruta, Stakišaitis Donatas, Valančiūtė Angelija, Balnytė Ingrida

*Department of Histology and Embryology, Faculty of Medicine,
Lithuanian University of Health Sciences, Lithuania*

Objectives. The study aimed to compare the effectiveness of sodium dichloroacetate (NaDCA) 10 mM with temozolomide (TMZ) 100 μ M on glioblastoma (GB) U87 MG and T98G cell tumor xenograft growth and the expression of PCNA, p53, and EZH2 in the tumor.

Materials and methods. U87 MG and T98G cell tumors were formed with 10^6 cells and type I Rat Tail Collagen, and grafted onto CAM of a fertilized Cobb-500 chicken egg. The study groups were: U87-10 mM NaDCA (n = 24), U87-100 μ M TMZ (n = 15), U87-control (non-treated GB, n = 20), T98G-10 mM NaDCA (n = 22), T98G-100 μ M TMZ (n = 11), T98G-control (non-treated, n = 12). Tumor invasion into CAM and structural changes were evaluated by biomicroscopy and stereomicroscopy with fluorescent dextran. Immunohistochemistry and light microscopy were used for the tumor morphological evaluation and identification of the tumor's PCNA, p53 and EZH2 expression.

Results. NaDCA and TMZ reduced U87 and T98G tumor invasion into CAM ($p \leq 0.02$), where TMZ had a greater effect. In the T98G tumor, 10 mM NaDCA and 100 μ M TMZ reduced CAM thickness ($p \leq 0.02$); 100 μ M TMZ also reduced the number of blood vessels in CAM under the tumor ($p = 0.002$). U87 tumor CAM thickness and a number of blood vessels were only inhibited by 100 μ M TMZ ($p \leq 0.0002$). Reduced neoangiogenesis in respective tumors' groups was confirmed by fluorescence microscopy. The 10 mM NaDCA reduced p53, PCNA and EZH2 expression in U87 tumor ($p \leq 0.002$); in T98G tumor, this dose reduced only p53 and EZH2 expression ($p < 0.0001$). The 100 μ M TMZ reduced p53, PCNA and EZH2 expression in U87 and T98G tumors ($p \leq 0.003$).

Conclusions. The study showed that NaDCA and TMZ were similar in their effectiveness in reducing tumor invasion and neoangiogenesis in U87 and T98G cell tumors.

The expression of collagen neoepitope C2C in the articular cartilage and its relation with joint tissue damage in patients with knee osteoarthritis

Torga Taavi¹, Suutre Siim¹, Kisand Kalle², Aunapuu Marina¹, Arend Andres¹

¹*Institute of Biomedicine and Translational Medicine, University of Tartu, Estonia*

²*Department of Internal Medicine, University of Tartu, Estonia*

Objectives. The aim of this study was to correlate the degree of articular cartilage damage in OA patients with C2C expression in histological samples of tissues removed during total knee replacement.

Materials and methods. Cartilage samples were obtained from 27 patients aged from 55 to 66 years. In each patient medial and lateral tibia plateau samples were analyzed according to the OARSI histopathology grading system. C2C expression was evaluated on histological slides by semi-quantitative analysis using ImageJ Fiji software.

Results. The C2C expression was found in all the regions of the articular cartilage (i.e. the superficial zone, mid zone, deep zone, tidemark area and the zone of calcified cartilage). Spearman's rank correlation analysis showed a significant positive correlation ($\rho = 0.289$, $P = 0.0356$) between the histological grade of tissue damage and the percentage of C2C staining. In addition, a highly significant positive correlation ($\rho = 0.388$, $P = 0.0041$) was found between the osteoarthritis score (combining the histological grade of damage with the OA macroscopic stage) and the percentage of C2C staining in the samples.

Conclusions. Our study suggests that local expression of C2C correlates with cartilage damage in the knee affected by OA. This further assures that C2C can be a perspective marker for the evaluation of pathological processes in OA course and OA clinical trials.

Radiological insights into chronic Pelvic Congestion Syndrome and May-Thurner Syndrome: a comparative study of selected cases in Latvia

Trošins Daniils¹, Kratovska Aina², Kažoka Dzintra³, Pilmane Māra³

¹ Faculty of Medicine, Rīga Stradiņš University, Latvia

² "RAKUS" Radiological center, Latvia

³ Institute of Anatomy and Anthropology, Rīga Stradiņš University, Latvia

Objectives. The study aimed to examine the relationship between Pelvic Congestion Syndrome (PCS), May-Thurner Syndrome (MTS), and the venous vascular changes that lead to these conditions and to investigate the frequency of PCS and MTS and compare them with asymptomatic anatomical variations.

Materials and methods. The case group comprised women diagnosed with pelvic congestion syndrome (PCS) and May-Thurner syndrome (MTS), while the control group comprised patients without these syndromes. The assessed risk factors included venous outflow obstruction (VOD and VOS), dilation of the internal iliac veins (VICS), and compression of the right common iliac artery. Radiological assessments were conducted to identify cases with over 70% strictures in the proximal segment of the left common iliac vein. Precise measurements were taken for the right ovarian vein at the fourth lumbar vertebra (L4) level and the left ovarian vein at the third lumbar vertebra (L3) level. CT images from RAKUS and the Radiology Centre's PACS database were used in the study. All CT scans were anonymized for retrospective analysis. The radiological images were processed using Intel Space Vascular Analysis and SECTRA PACS software for database and statistical analysis.

Results. VOS was statistically significantly different between groups of MTS patients and the control group (Mann-Whitney: $U = 177$, $p = 0.001$). Also, findings showed statistically significant differences between patients with asymptomatic increased VOS and the control group (Mann-Whitney: $U = 941.5$, $p = 0.001$) in VOD measurements. A weak correlation was observed between the VOS and VOD measurements in the control group ($r(53)$, $p = 0.028$). There was a statistically significant difference between the 18–30 and 46–60 age groups in VICS congestion before the youngest group (Kruskal-Wallis: $p = 0.016$).

Conclusions. The two syndromes significantly impact anatomical features and the venous system. Further research using venography and MRI to diagnose Pelvic Congestion Syndrome is essential for acquiring more precise data.

Analysis of indices of children's physical development in a longitudinal study

Umbraško Silvija¹, Martinsone-Bērzkalne Liene¹, Edelmers Edgars¹, Asare Lāsma²

¹*Institute of Anatomy and Anthropology, Rīga Stradiņš University, Latvia*

²*Statistics Unit, Rīga Stradiņš University, Latvia*

Objectives. The aim of this study is to evaluate key indices of physical development, specifically Body Mass Index (BMI) and the Bruggs Index, in children from birth to 17 years.

Materials and methods. A longitudinal case analysis of 70 children (35 girls and 35 boys) was conducted. BMI and the Bruggs Index were tracked and analyzed over the course of childhood and adolescence. The study protocol was approved by the RSU Ethics Committee (2-PEC-4/597/2022). Measurements were taken by the RSU Anthropology Laboratory. Relative indices were used to express proportional relationships between different body measures.

Results. For girls, mean BMI values from birth to 11 years ranged from 13.6 to 18.0, below normal, and from 18.6 to 22.2 between ages 12 to 17, within the normal range. Boys' BMI values from birth to 10 years ranged from 13.8 to 18.4, below normal, and from 19.0 to 23.4 for ages 11 to 17. The Bruggs Index showed the chest was wide from birth to 4 years, normal from 4 to 7, narrow from 7 to 14, and normal again from 14 to 17 years.

Conclusions. Girls' BMI showed the greatest increase from birth to 1 year and 10 to 11 years. Boys' BMI increased most from 13 to 14 years. Peak BMI changes occurred for girls at 12–13 years and boys at 13–14 years.

Distribution of immunomodulation, protection and regeneration factors in cleft affected bone and cartilage

Vaivads Mārtiņš, Pilmane Māra

*Department of Morphology, Institute of Anatomy and Anthropology,
Rīga Stradiņš University, Latvia*

Objectives. Orofacial clefts can cause a significant defect in the underlying supportive tissue, which can disturb normal tissue homeostasis and remodeling processes. Multiple tissue factors can affect local immune response, provide protection and tissue growth regulation. Some of them have not been well studied in cleft affected supportive tissue like galectin-10 (Gal-10), nuclear factor kappa-light-chain-enhancer of activated B cells protein 65 (NF- κ B p65), heat shock protein 60 (HSP60) and 70 (HSP70), cathelicidin (LL-37) while regeneration factors like type I collagen (Col-I) and bone morphogenetic proteins 2 and 4 (BMP-2/4) have not been evaluated together with immunomodulation and protection factors. The information about the distribution and interactions between these factors could improve the understanding of cleft affected supportive tissue regeneration and healing potential after surgery.

Materials and methods. This study used immunohistochemistry with the semiquantitative counting method to detect and evaluate Gal-10, NF- κ B p65, HSP60, HSP70, LL-37, Col-I, and BMP-2/4 containing cells in control tissue and cleft affected supportive tissue to determine the differences in factor distribution between healthy supportive tissue and cleft affected bone and cartilage. Patients and controls were subdivided into four groups with 5 individuals in each group (all mixed dentition age) – 2 control groups for bone tissue and cartilage, respectively and 2 cleft affected supportive tissue groups.

Results. Evaluated tissue factors were found in each study group. Multiple statistically significant correlations between factor positive cells were calculated.

Conclusions. The number of HSP70 positive cells was significantly increased in cleft affected cartilage which could indicate that HSP70 could provide protective action in cleft affected supportive tissue against stressors. The significant increase of Col-I positive osteocytes in cleft affected bone was also noted, which might indicate increased osteocyte activity and bone remodeling process. Correlations between factors indicate notable differences in molecular interactions between healthy and cleft affected supportive tissue.

Chronic stress impact on pancreas morphology in type 1 diabetes mellitus

Vosyliūtė Rūta¹, Achahbar Charki Hiba², Šimkūnaitė-Rizgeliene Renata¹, Bikulčienė Inga³,
Baleišis Justinas³, Rudys Romualdas³, Tutkuvienė Janina¹

¹Department of Anatomy, Histology and Anthropology, Institute of Biomedical
Sciences, Faculty of Medicine, Vilnius University, Lithuania

²Faculty of Medicine, Vilnius University, Lithuania

³Department of preclinical research, Centre for Innovative Medicine and Department of Physiology,
Biochemistry, Microbiology and Laboratory Medicine, Institute of Biomedical Sciences,
Faculty of Medicine, Vilnius University, Lithuania

Objectives. The aim of this study was to evaluate the impact of chronic psychological stress on the pancreatic tissue in type 1 diabetes mellitus (T1DM).

Materials and methods. 35 mature healthy Wistar rats were randomly assigned and housed into 4 groups: the Control group, Stress group, T1DM group, and T1DM+Stress group. 28 days of restrain stress was applied for two hours each day. A single dose of 65 mg/kg of streptozotocin treatment was used to establish diabetes using the procedure. On the 29th day of the experiment, rats were anesthetized. Pancreas were removed and prepared for histological analysis. 7 samples were analyzed for the Control group, 8 for the Stress group, 11 for the T1DM and 7 for T1DM+Stress group. Samples were analyzed using the QuPath (Version 0.4.4) program by measuring the endocrine part with total pancreatic tissue ratio. SPSS program was used for statistical analysis. The Kruskal-Wallis test was used to determine differences in the median of endocrine part between the four groups.

Results. Percentage of endocrine part in a total area of pancreatic tissue median of the Control group was 0.96 (min: 0.52; max: 1.77); the Stress group – 0.41 (0.23; 0.93); T1DM group – 0.45 (0.09; 1.64); T1DM+Stress group – 0.23 (0.08; 0.46). A notable difference was between the medians of Control vs. Stress group, suggesting that stress may have a significant impact on the measured outcome. The Control group had a higher median value, indicating better outcomes compared to the Stress group ($p = 0.017$). There was a significant difference between Control and T1DM groups, where p was 0.014. But the highest difference was between Control and T1DM+Stress group, with a p value < 0.001 .

Conclusions. The pancreas, which plays a crucial role in regulating blood sugar levels by producing insulin, may become overworked and less effective under stress. A combination of T1DM and stress may worsen the condition or outcome being measured.

Authors

A

Achahbar Charki, Hiba	96
Akota, Ilze	52, 62
Alčauskaitė, Justina	90
Allmang, Cristin	28
Almonaitiene, Ruta	50
Apele, Zane	58
Arend, Andres	79, 92
Asare, Lāsma	59, 78, 94
Aukštikalnienė, Rasa	90
Aunapuu, Marina	79, 92

B

Babal, Pavel	19
Babenko, Tetiana	68
Baleišis, Justinas	96
Balnytė, Ingrida	64, 66, 72, 91
Barkus, Arunas	43, 49, 50
Bartuškienė, Violeta	46
Batulevičius, Darius	24
Benes, Michal	32
Bikulčienė, Inga	96
Bode, Mārtiņš	60
Brikune, Elizabete	61
Buile, Dace	62

C

Čepulienė, Ramune	46, 63
-------------------	--------

D

Dabužinskiene, Anita	77
Damanskienė, Eligija	64
Dambergs, Kristaps	25
Derbeņeva, Darja	65
Diržiuvienė, Raminta	66
Dorichevska, Raisa	68
Drożdż, Adrian	45
Drutowska, Andzelika	83
Dūrītis, Ilmārs	28
Dursun, Erdinc	21

E

Edelmers, Edgars	26, 67, 94
------------------	------------

F

Fedirko, Pavlo	14, 68
Fišere, Inese	67

G

Gardovskis, Jānis	84
Garkava, Natalia	68
Gasiliunas, Donatas	77
Gervickaite, Simona	43, 49, 50
Gezen Ak, Duygu	21
Gontar, Lukasz	83
Gorodetsky, Michael Lior	81
Grabčika, Arta	69
Green, Tami	70
Groma, Valerija	27, 42, 80
Gunhaga, Lena	70

H

Herma, Tomas	32
Hussar, Piret	28

I

Inokaitis, Hermanas	29
Isakova, Jelena	30
Ivanovs, Andrejs	15, 59

J

Jakimaviciene, Egle Marija	30
Jakovļevs, Arvids	71
Jankauskas, Rimantas	35
Järveots, Tõnu	28
Juknevičienė, Milda	72
Junga, Anna	31, 85
Juodziukyniene, Nomedā	77

K

Kachlik, David	32
Kadiša, Anda	42
Kaiser, Radek	32
Kažoka, Dzintra	33, 56, 60, 69, 73, 74, 75, 84, 93
Khadanovich, Anhelina	32
Khmel, Olena	40, 41
Kilimaitė, Evelina	81
Kisand, Kalle	92
Kochanski, Maksymilian	83
Kozakaitė, Justina	35
Kratovska, Aina	93
Kuļibaba, Georgijs	75

L

Lapeikis, Ignas	76
Lapides, Lenka	19
Lasiene, Kristina	66, 77

Laurinavičiūtė, Guoda	46	Šinkarevs, Staņislavs	47, 48
Lekšas, Mindaugas	81	Skredenieni, Ruta	91
Levin, Denis	24	Skrīde, Andris	56
Lohova, Elizabeta	83	Skrīpka, Valdas	24
M		Skrīpkienė, Gertrūda	24
Malinauskas, Mantas	76	Skuja, Sandra	27, 42, 80
Martinsonė-Bērzkalne, Liene	78, 94	Skujienė, Grita	90
Melderis, Ivars	83	Šlažaitė, Gerda	46
Merkurjeva, Kristine	34, 51	Šlekiene, Lina	66, 70
Mialkowskyj, Damian	35	Sokolovska, Lība	42
Miliauskienė, Zydrune	63	Spārītis, Ojārs	18
Misiute, Agne	36	Sperga, Māris	47
N		Stakišaitis, Donatas	64, 66, 72, 91
Namm, Aimar	79	Stasiunas, Augustinas	30
Naumovs, Vladimirs	27, 80	Strance, Ģertrūde	60
Nedzinskiene, Laura	36, 63	Streļčenko, Jekaterina	46
Novikova, Jekaterina	87	Štrumfa, Ilze	34, 47, 48, 51
O		Štrumfs, Boriss	34, 47, 48, 51
Onashko, Yulia	40	Studers, Pēteris	42
Ozola, Laura	37	Stukaite-Ruibiene, Egle	43, 50
P		Sumerags, Dins	44
Palubinskienė, Jolita	66, 81	Suutre, Siim	92
Paulikaitė, Edita	90	Szeliga, Stanisław	45
Pauliņš, Arvis	82	T	
Pauža, Dainius Haroldas	16, 29, 40, 41, 89	Torga, Taavi	79, 92
Paužienė, Neringa	29, 39, 41, 76, 87	Trošins, Daniils	93
Pētersons, Aigars	55, 65, 84, 85	Tutkus, Jonas	43, 49, 50
Pilmane, Māra	14, 25, 31, 33, 37, 38, 44, 52, 54, 55, 56, 58, 61, 62, 65, 68, 73, 74, 82, 83, 84, 85, 88, 93, 95	Tutkus, Vytautas	63
Piombino-Mascalì, Dario	35	Tutkuvienė, Janina	30, 36, 43, 46, 49, 50, 63, 96
Pivriķa, Evelīna	85	U	
Pļaviņa, Liāna	86	Uljanovs, Romans	34, 48, 51
Polgūj, Michał	17	Umbraško, Silvija	78, 94
Popvska-Percinic, Florina	28	V	
Prieto-Simon, Beatriz	83	Vaivads, Mārtiņš	52, 95
R		Valančiūtė, Angelija	64, 66, 72, 91
Radzeviciute, Simona	77	Varga, Ivan	19
Ranceviene, Dalia	39, 41	Vētra, Jānis	53, 59, 69, 84
Reivytytė, Rosita	46	Vidusa, Līga	34, 51
Rekke, Kirsten	40, 41	Vīksne, Rūdolfs Jānis	54
Rone, Alise Elizabete	88	Virbauskytė, Viktorija	46
Rudys, Romualdas	96	Vosyliūtė, Rūta	46, 63, 96
Rysevaite-Kyguoliene, Kristina	39, 40, 41, 76, 87, 89	W	
S		Winkelmann, Andreas	20
Sabeckis, Ignas	39, 40, 89	Y	
Saburkine, Inga	41	Yilmazer, Selma	21
Segliņa, Gunta	25, 44, 54	Z	
Semenistaja, Sofija	42	Žalgevičienė, Violeta	46, 90
Semenkovaite, Justina	46	Zariņa, Kaiva Zīle	55
Sėrikovaitė, Evita	90	Zicāns, Matīss	56
Šimkūnaitė-Rizgelienė, Renata	43, 46, 49, 50, 63, 96	Zilaitiene, Birute	77



RĪGA STRADIŅŠ
UNIVERSITY

Address: Dzirciema street 16, Rīga, Latvia,
LV-1007

E-mail: rsu@rsu.lv
www.rsu.lv

INSTITUTE OF ANATOMY AND ANTHROPOLOGY

Address: Kronvalda blvd. 9, Rīga, Latvia,
LV-1010

Phone: + 371 68414740

E-mail: aai@rsu.lv

www.rsu.lv/en/institute-anatomy-and-anthropology

ISBN 978-9934-618-58-1



9 789934 618581 >